

1 HESS 2015-325 - Changes to Manuscript

2 6/20/2016

3 After acceptance by the editor with no suggested changes (manuscript-version3.pdf) I updated  
4 some references, corrected a reference's name, and added first names to the author list on the  
5 title page. Page numbers/line numbers refer to final unmarked manuscript.

- 6 • Page 1 – lines 3-4 – added first names to authors
- 7 • Page 4-lines 64,74,76; Page 4 lines 95; Page 26-lines 682,684; Page 28-line 761 – added  
8 umlaut to reference last name Blöschl. I had forgotten to modify this earlier.
- 9 • Page 7-lines 166-167 – A colleague pointed out I was missing a reference to the  
10 NHDPlus dataset, added reference on page 7 (lines 166-167) and in the final references  
11 list (Page 32, lines 827-829)
- 12 • Page 26, lines 667-670 – finalized this reference (was in review status in earlier version)
- 13 • Page 27, lines 689-691 and lines 692-693 – added doi numbers for these two referencs
- 14 • Page 28, lines 711-713 – Fixed incorrect formatting of reference, added doi number.

15  
16  
17  
18  
19  
20  
21  
22  
23  
24  
25

26 **Parameter regionalization of a monthly water balance model for**  
27 **the conterminous United States**

---

28 **Andrew R. Bock<sup>1</sup>, Lauren E. Hay<sup>2</sup>, Gregory J. McCabe<sup>2</sup>, Steven L. Markstrom<sup>2</sup>, and R.**  
29 **Dwight Atkinson<sup>3</sup>**

Comment [Bock1]: Full first names of authors

30 <sup>1</sup> U.S. Geological Survey, Colorado Water Science Center, Denver Federal Center, P.O. Box  
31 25046, MS 415, Denver, Colorado, 80225, USA

32 <sup>2</sup> U.S. Geological Survey, National Research Program, Denver Federal Center, P.O. Box 25046,  
33 MS 413, Denver, Colorado, 80225, USA

34 <sup>3</sup> U.S. Environmental Protection Agency, Office of Water (4503-T), 1200 Pennsylvania Ave.,  
35 Washington, DC, 20004, USA

36

37 Correspondence to: A. Bock (abock@usgs.gov)

38

39

40

41

42

43

44

45

46

47

48

49

50

51

52 **Abstract**

53 A parameter regionalization scheme to transfer parameter values from gaged to ungaged areas  
54 for a monthly water balance model (MWBM) was developed and tested for the conterminous  
55 United States (CONUS). The Fourier Amplitude Sensitivity Test, a global-sensitivity algorithm,  
56 was implemented on a MWBM to generate parameter sensitivities on a set of 109,951 hydrologic  
57 response units (HRUs) across the CONUS. The HRUs were grouped into 110 calibration  
58 regions based on similar parameter sensitivities. Subsequently, measured runoff from 1,575  
59 streamgages within the calibration regions were used to calibrate the MWBM parameters to  
60 produce parameter sets for each calibration region. Measured and simulated runoff at the 1,575  
61 streamgages showed good correspondence for the majority of the CONUS, with a median  
62 computed Nash-Sutcliffe Efficiency coefficient of 0.76 over all streamgages. These methods  
63 maximize the use of available runoff information, resulting in a calibrated CONUS-wide  
64 application of the MWBM suitable for providing estimates of water availability at the HRU  
65 resolution for both gaged and ungaged areas of the CONUS.

66

67

68

69

70

71

72

73

74

75

76 **1 Introduction**

77 The WaterSMART program (<http://water.usgs.gov/watercensus/WaterSMART.html>) was started  
78 by the United States (U.S.) Department of the Interior in February 2010. Under WaterSMART,  
79 the National Water Census (NWC) was proposed as one of the U.S. Geological Survey's (USGS)  
80 key research directions with a focus on developing new hydrologic tools and assessments. One  
81 of the major components of the NWC is to provide estimates of water availability at a sub-  
82 watershed resolution nationally (<http://water.usgs.gov/watercensus/streamflow.html>) with the  
83 goal of determining if (1) the Nation has enough freshwater to meet both human and ecological  
84 needs and (2) this water will be available to meet future needs. Streamflow measurements do not  
85 provide direct observations of water availability at every location of interest; approximately 72  
86 percent (%) of land within the conterminous U.S. is gaged, with approximately 13% of these  
87 gaged areas being unaffected by anthropogenic effects (Kiang et al., 2013). This creates the  
88 challenge of determining the best method to transfer information from gaged catchments to data-  
89 poor areas where results cannot be calibrated or evaluated with measured streamflow (Vogel,  
90 2006). This transfer of model parameter information from gaged to ungaged catchments is  
91 known as hydrologic regionalization (Blöschl and Sivapalan, 1995).

Comment [Bock2]: Added umlaets to Blöschl

92 Many hydrologic regionalization methods have focused on developing measures of similarity  
93 between gaged and ungaged catchments using spatial proximity and physical characteristics.  
94 These methods are highly dependent on the complexity of the terrain and scale at which the  
95 relations are derived. Spatial proximity is considered the primary explanatory variable for  
96 hydrologic similarity (Sawicz et al., 2011) because of the first-order effects of climatic and  
97 topographic controls on hydrologic response. Close proximity, however, does not always result  
98 in hydrologic similarity (Vandewiele and Elias, 1995; Smakhtin, 2001; Ali et al., 2012).

99 Physical characteristics have been used as exploratory variables to develop a better  
100 understanding of the relation between model parameters that represent model function, and  
101 physical properties of the catchment (Merz and Blöschl, 2004). The relation between model  
102 parameters and the relevant physical characteristics, expressed for example as a form of  
103 multivariate regression, can be transferred to ungaged catchments (Merz and Blöschl, 2004).  
104 Model parameter definitions are by nature ambiguous and often difficult to correlate to a small

105 number of meaningful variables such as physical and climatic characteristics (Zhang et al.,  
106 2008); some studies have found no significant correlation between catchment attributes and  
107 model parameters (Seibert, 1999; Peel et al., 2000), whereas others found that high correlation  
108 does not guarantee parameters that result in reliable model simulations of measured data (Sefton  
109 and Howarth, 1998; Kokkonen et al., 2003; Oudin et al., 2010). Physical characteristics also are  
110 used to classify catchments into discrete regions or clusters based on similarity in multi-  
111 dimensional attribute space (Oudin et al, 2008, 2010; Samuel et al., 2011). While these methods  
112 have indicated some success in simulating behavior of specific hydrologic components, such as  
113 base flow (Santhi et al., 2008), other efforts utilizing discrete clusters performed poorly in  
114 explaining variability of measured streamflow (McManamay et al., 2011).

115 Two important components of the transfer of parameters to ungauged catchments are the  
116 identification of (1) influential (and non-influential) parameters, and (2) geographic extents and  
117 scales at which parameters exert control on model function. Reducing the number of parameters  
118 is important for calibration efficiency by reducing the structural bias of the model and the  
119 uncertainty of results where they cannot be verified or confirmed (van Griensven et al., 2006). A  
120 high number of calibrated, poorly constrained parameters can often mask data or structural  
121 errors, which can go undetected and reduce the skill of the model in replicating results outside of  
122 calibration conditions (Kirchner, 2006; Blöschl et al., 2013). This increases the potential for  
123 equifinality of parameter sets and higher model uncertainty that can be propagated to model  
124 results (Troch et al., 2003).

125 Sensitivity analysis (SA) has advanced the understanding of parameter influence on model  
126 behavior and structural uncertainty. SA measures the response of model output to variability in  
127 model input and/or model parameter values. SA partitions the total variability in the model  
128 response to each individual model parameter (Reusser et al., 2011) and results in a more-defined  
129 set of parameters and parameter ranges. Identification of sensitive parameters and their ranges is  
130 important for hydrologic model applications as key model parameters can vary spatially across  
131 physiographic regions, and also temporally (Tang et al., 2007; Guse et al., 2013).

132 Until recently, the high computational demands of SA have limited most implementations of  
133 hydrologic model SA to local sensitivity algorithms that evaluate a single parameter at a time

134 (Tang et al., 2007). Global SA uses random or systematic sampling designs of the entire  
135 parameter space to quantify variation in model output (van Griensven et al. 2006, Reusser et al.  
136 2011). Some of these methods can account for parameter interaction and quantify sensitivity in  
137 non-linear systems. Global SA methods are computationally intensive (Cuo et al., 2011), but  
138 ever increasing computational efficiency has allowed for the development and application of a  
139 large number of global SA algorithms.

140 Previous work has suggested that isolating the key parameters that control model performance  
141 can be used to infer dominant physical processes in the catchment, as well as which components  
142 of the model dominate hydrologic response (van Griensven et al. 2006, Tang et al., 2007,  
143 Reusser et al., 2011). To date, there has been little analysis of the use of SA for deriving  
144 measures of hydrologic similarity across catchments that can be applied towards hydrologic  
145 regionalization of model parameters. The spatially-distributed application of SA could be used  
146 to provide additional information for the delineation of homogeneous regions for parameter  
147 transfer based on similarity of model results from the SA. This strategy allows for the use of the  
148 existing model information and configuration to develop a calibration and regionalization  
149 framework without significantly changing the model structure or implementation

150 In this study, we present a hydrologic regionalization methodology for the CONUS that derived  
151 regions of hydrologic similarity based on the response of a Monthly Water Balance Model  
152 (MWBM) to parameter SA. Groups of streamgages within each region are calibrated together to  
153 define a single parameter set for each region. By extending model calibration to a large number  
154 of sites grouped by similarity through a quantified measure of model behavior, a more specific  
155 and constrained parameter space that fits each region can be identified.

## 156 **2 Methods**

### 157 **2.1 Monthly Water Balance Model**

158 The MWBM (Fig. 1) is a modular accounting system that provides monthly estimates of  
159 components of the hydrologic cycle by using concepts of water supply and demand (Wolock and  
160 McCabe 1999; McCabe and Markstrom, 2007). Monthly temperature (T) is used to compute  
161 potential evapotranspiration (PET) and to partition monthly precipitation (P) into rain and snow

162 (Fig. 1). Precipitation that occurs as snow is accumulated in a snow pack (snow storage as snow  
163 water equivalent, or SWE); rainfall is used to compute direct runoff ( $R_{\text{direct}}$ ) or overland flow,  
164 actual evapotranspiration (AET), soil-moisture storage recharge, and surplus water, which  
165 eventually becomes runoff (R) (Fig. 1). When rainfall for a month is less than PET, AET is equal  
166 to the sum of rainfall, snowmelt, and the amount of moisture that can be removed from the soil.  
167 The fraction of soil-moisture storage that can be removed as AET decreases linearly with  
168 decreasing soil-moisture storage; that is, water becomes more difficult to remove from the soil as  
169 the soil becomes drier and less moisture is available for AET. When rainfall (and snowmelt)  
170 exceeds PET in a given month, AET is equal to PET; water in excess of PET replenishes soil-  
171 moisture storage. When soil-moisture storage reaches capacity during a given month, the excess  
172 water becomes surplus and a fraction of the surplus ( $R_{\text{surplus}}$ ) becomes R, while the remainder of  
173 the surplus is temporarily held in storage. The MWBM has been previously used to examine  
174 variability in runoff over the CONUS (Wolock and McCabe, 1999; Hay and McCabe 2002;  
175 McCabe and Wolock, 2011a) and the global extent (McCabe and Wolock, 2011b). Table 1 lists  
176 the MWBM parameters, with definitions and parameter ranges for calibration.

177 The *Ppt\_adj* and *Tav\_adj* parameters specify seasonal adjustments for precipitation and  
178 temperature, respectively. The seasonal adjustment parameters were included to account for  
179 errors in the precipitation and temperature data used in this analysis. Sources of systematic and  
180 non-systematic errors of climate forcing data are well documented from the precipitation gage-  
181 derived sources (Groisman and Legates, 1994; Adam and Lettenmaier, 2003). Interpolation of  
182 these systematic errors from point-scale to gridded domains may propagate these biases,  
183 especially in complex terrain (Clark and Slater, 2006; Oyler et al, 2015). The use of adjustment  
184 factors allows uncertainty associated with forcing data and model parameter values to be treated  
185 separately (Vrugt et al., 2008).

186 *Figure 1. Conceptual diagram of the Monthly Water Balance Model (McCabe and Markstrom*  
187 *2007). Processes influenced by model parameters used in Fourier Amplitude Sensitivity Test*  
188 *(FAST) those identified by green arrow and numbered 1-5 (Table 1).*

189 *Table 1. Monthly Water Balance Model parameters and ranges.*

190 The MWBM was applied to the CONUS with 109,951 hydrologic response units (HRUs) from  
191 the Geospatial Fabric (Viger and Bock, 2014), a national database of hydrologic features for  
192 national hydrologic modeling applications (Fig. 2). This HRU derivation is based on an  
193 aggregation of the NHDPlus dataset (U.S. Environmental Protection Agency and U.S.  
194 Geological Survey, 2010), an integrated suite of geospatial data that incorporates features from  
195 the National Hydrography Dataset (<http://nhd.usgs.gov/>), the National Elevation Dataset  
196 (<http://ned.usgs.gov/>), and the Watershed Boundary Dataset (<http://nhd.usgs.gov/wbd.html>). The  
197 sizes of the HRUs range from less than 1 square kilometer (km<sup>2</sup>) up to 67,991 km<sup>2</sup>, with an  
198 average size of 74 km<sup>2</sup>.

Comment [Bock3]: Added reference

199 Inputs to the MWBM by HRU are: (1) monthly P (millimeters), monthly mean T (degrees  
200 Celsius), (2) latitude of the site (decimal degrees), (3) soil moisture storage capacity  
201 (millimeters), and (4) monthly coefficients for the computation of PET (dimensionless).  
202 Monthly P and mean T were derived from the daily time step, 1/8° gridded meteorological data  
203 for the period of record from January 1949 through December 2011 (Maurer et al., 2002).  
204 Monthly P and T data were aggregated for each HRU using the USGS Geo Data Portal  
205 (<http://cida.usgs.gov/climate/gdp/>) (Blodgett et al., 2011). Latitude was computed from the  
206 centroid of each HRU. Soil moisture storage capacity was calculated using a 1 km<sup>2</sup> grid derived  
207 from the Soils Data for the Conterminous United States (STATSGO) (Wolock, 1997). The  
208 monthly PET coefficients were calculated by calibrating the Hamon PET values to Farnsworth et  
209 al. (1982) mean monthly free-water surface evapotranspiration. McCabe et al. (2015) describes  
210 these PET coefficient calculations in detail.

211 *Figure 2. Hydrologic Response Units of the Geospatial Fabric, differentiated by color, overlain*  
212 *by NHDPlus region boundaries (R01-R18).*

## 213 **2.2 Fourier Amplitude Sensitivity Test**

214 A parameter SA for the CONUS was conducted for the MWBM using the Fourier Amplitude  
215 Sensitivity Test (FAST) to identify areas of hydrologic similarity. FAST is a variance-based  
216 global sensitivity algorithm that estimates the contribution to model output variance explained by  
217 each parameter (Cukier et al. 1973, 1975; Saltelli et al. 2000). Advantages of using FAST over



218 other SA methods are that FAST can calculate sensitivities in non-linear systems, and is  
219 extremely computationally efficient. The seasonal adjustment factors were not incorporated into  
220 the FAST analysis. We viewed the seasonal adjustment factors as more related to the forcing  
221 data, and for this application only parameters associated with model structure were included  
222 (first five parameters in Table 1).

223 FAST transforms a model's multi-dimensional parameter space into a single dimension of  
224 mutually independent sine waves with varying frequencies for each parameter, while using the  
225 parameter ranges to define each wave's amplitude (Cukier et al. 1973, 1975; Reusser et al.  
226 2011). This methodology creates an ensemble of parameter sets numbering from 1 to N, each of  
227 which is unique and non-correlated with the other sets. Parameter sets are derived using the  
228 corresponding y-values along each parameter's sine wave given a value on the x-axis. The  
229 model is executed for all parameter sets using identical climatic and geographic inputs for each  
230 simulation. The resulting series of model outputs are Fourier-transformed to a power spectrum  
231 of frequencies for each parameter. Parameter sensitivity is calculated as the sum of the powers  
232 of the output variance for each parameter, divided by the sum of the powers of all parameters  
233 (Total Variance). The parameter sensitivities are scaled so that the sensitivities for all  
234 parameters sum to 1. Thus, parameters that explain a large amount of variability in the model  
235 output have higher (i.e. closer to 1) parameter sensitivity values.

236 FAST was implemented with the MWBM using the 'fast' library in the statistical software R  
237 (Reusser, 2012; R Core Team, 2013). Parameter ranges used by FAST for generating wave  
238 amplitudes of parameter ensembles across the CONUS were based on table 1. The 'fast' R  
239 package pre-determines the minimal number of runs necessary to estimate the sensitivities for  
240 the given number of parameters (Cukier et al., 1973). For our application we generated an  
241 ensemble of 1000 parameter sets (as compared to the minimally suggested number of 71  
242 estimated by 'fast'). The use of the minimal number of parameter sets should be a consideration  
243 for more complex models, but the relative computational efficiency and parallelization of the  
244 MWBM allowed the model to simulate this larger number of parameter sets quickly to help  
245 ensure a robust parameter sensitivity analysis.

246 Many applications of SA in hydrologic modeling have evaluated parameter sensitivity for  
247 measured streamflow using performance-based measures such as bias, root mean squared error  
248 (RMSE), and the Nash-Sutcliffe Efficiency (NSE) (Nash and Sutcliffe, 1970; Moriasi et al.,  
249 2007). In this study, parameter sensitivity is examined using two hydroclimatic indices that  
250 account for the magnitude and variability of both climatic input and model output: the (1) Runoff  
251 Ratio (RR), a ratio of simulated runoff to precipitation, and (2) Runoff Variability (RV) index,  
252 the standard deviation of simulated runoff to the standard deviation of precipitation  
253 (Sankarasubramanian and Vogel, 2003).

### 254 **3 Parameter regionalization procedure**

255 The following sections describe the workflow for the MWBM calibration and regionalization  
256 (illustrated in Figure 3). The MWBM parameter sensitivities from the FAST analysis were  
257 evaluated across the CONUS. The spatial patterns and magnitudes of parameter sensitivities  
258 were used to organize the 109,951 HRUs into hydrologically similar regions referred to in the  
259 paper as calibration regions. During the initial streamgage selection, potential streamgages were  
260 identified for use in the grouped MWBM calibration. These selected streamgages then were  
261 individually calibrated. Using a number of selection criteria, a final set of calibration gages were  
262 derived within each calibration region. The grouped MWBM calibration produced an ‘optimal’  
263 set of MWBM parameters for each calibration region by evaluating simulated MWBM variables  
264 converted to Z-scores.

265 *Figure 3. Schematic flowchart of the parameter regionalization procedure described in Section*  
266 *3: Parameter sensitivities (3.1), Calibration regions (3.2), Initial streamgage selection (3.3),*  
267 *and Grouped streamgage calibration (3.4).*

#### 268 **3.1 Parameter sensitivities**

269 The relative sensitivities derived from the FAST analysis using the RR and RV indices at each of  
270 the 109,951 HRUs across the CONUS were scaled so that the five MWBM parameter  
271 sensitivities derived for each HRU summed to 100 (Fig. 4). RR (Fig. 4a) is most sensitive to the  
272 parameter *Drofac* in regions where MWBM runoff is not dominated by snowmelt and orographic  
273 precipitation, such as arid and sub-tropical areas of the CONUS. MWBM parameters that

274 control snowpack accumulation and melt (*Meltcoef*, *Tsnow*, and *Train*) are more important to the  
275 RR in the extensive mountain ranges in the Western CONUS, and northerly latitudes around the  
276 Great Lakes and in the Eastern CONUS. The RR indicates the highest sensitivity to the *Rfactor*  
277 parameter in mountainous areas of the CONUS and areas of the West Coast, and moderate to  
278 high sensitivity in areas where the sensitivity of RR to *Drofac* is low. *Tsnow*, *Train*, and  
279 *Meltcoef* all share similar patterns across the CONUS. The spatial variability of the sensitivity of  
280 RR to *Meltcoef* indicates different physical mechanisms controlling *Meltcoef* parameter influence  
281 on RR in different areas of the CONUS. In the Western CONUS, the sensitivity of RR to  
282 *Meltcoef* is greatest in mountainous areas that accumulate and hold snowpack through the late  
283 spring, such as the Rocky Mountains, Cascade, and Sierra Nevada mountain ranges. In the  
284 Eastern and Midwestern CONUS, the sensitivity of RR to *Meltcoef* is greatest for HRUs with  
285 more northerly latitudes.

286 *Figure 4. Relative sensitivity of the (a) Rainfall Ratio (RR) and (b) Runoff Variability (RV)*  
287 *indices to Monthly Water Balance Model parameters.*

288 The spatial patterns of sensitivities of RV to the five MWBM parameters (Fig. 4b) show both  
289 similarities and deviations from the patterns shown in the RR maps. For the central part of the  
290 CONUS, the relative sensitivity for the parameter *Drofac* is high for both indices, and low for the  
291 parameter *Rfactor* for both indices. *Meltcoef*, *Tsnow*, and *Train* share the same relations between  
292 higher sensitivity and higher elevation (primarily in the western part of the CONUS), and higher  
293 sensitivity and more northerly latitude (primarily in the eastern half of the CONUS) for both  
294 indices. However, *Drofac* and *Rfactor* show distinctly different patterns of relative sensitivities  
295 for the eastern part of the CONUS for RV as compared to RR. The other three parameters  
296 follow the same general spatial patterns for RV as compared to RR, but with greater fine-scale  
297 spatial variation and patchiness. The differences between the spatial distributions of the  
298 sensitivities between the two indices highlight that applying SA to different model outputs can  
299 generate different levels of sensitivities for each parameter. In addition, the choice of objective  
300 function or model output for which to measure parameter sensitivity is important, as parameter  
301 sensitivities will differ depending on whether a user evaluating measures of magnitude, the  
302 variability of distribution, or timing (Krause et al., 2005; Kapangaziwiri et al, 2012).

303 Figure 5 illustrates the variability of parameter sensitivities between NHDPlus regions 08 (Lower  
304 Mississippi) and 14 (Upper Colorado) (see Fig. 2) for the RR and RV indices, and between the  
305 RR and RV within a single region. The Lower Mississippi and Upper Colorado NHDPlus  
306 regions have a similar number of HRUs (4,449 and 3,879, respectively) and cover a similar area  
307 (26,285 and 29,357 km<sup>2</sup>, respectively). The Lower Mississippi region has homogenous  
308 topography, with humid, subtropical climate, while the Upper Colorado region has highly  
309 variable topography, and thus highly variable climatic controls on hydrologic processes. For the  
310 Lower Mississippi region only one parameter dominates modeled RV variance (*Rfactor*, Fig. 5a)  
311 and modeled RR variance (*Drofac*, Fig. 5c). In contrast, for the Upper Colorado River region  
312 several parameters influence RV variability (*Drofac*, *Rfactor* and *Meltcoef*, Fig. 5b) and RR  
313 variability (*Drofac* and *Meltcoef*, Fig. 5d). In the Lower Mississippi Region the amount of  
314 snowfall is negligible, so the three parameters that control snowfall and snowpack accumulation  
315 in the MWBM have a negligible effect on the volume and variability of simulated total runoff.  
316 The *Rfactor* parameter controls almost all of the variance for the RV in the Lower Mississippi  
317 region. In humid, sub-tropical hydroclimatic regimes of the CONUS, peak runoff is coincident  
318 with peak precipitation, which is significant because these periods are when the surplus runoff is  
319 greatest. In the Upper Colorado, peak runoff is not coincident with peak precipitation, and the  
320 MWBM snow parameters have more control in modulating the variability and timing of runoff  
321 from snowmelt in the higher elevation HRUs. The comparison of the parameter sensitivities for  
322 these two regions illustrates how variable parameter sensitivities differ by region (i.e. different  
323 climatic and physiographic regions) and components of model response (i.e. volume and  
324 variability).

325 *Figure 5. Parameter sensitivities of Runoff Variability (RV; a-b) and Runoff Ratio (RR; c-d)*  
326 *indices for Monthly Water Balance Model parameters in the Lower Mississippi (R08) and*  
327 *Upper Colorado (R14).*

### 328 **3.2. Calibration regions**

329 The spatial patterns and magnitudes of parameter sensitivities across the CONUS were used as a  
330 basis for organizing HRUs into hydrologically similar regions for parameter regionalization  
331 through MWBM calibration. This idea is rooted in the hypothesis that geographically proximate

332 HRUs share similar forcings and conditions, and thus will behave similarly. This application  
333 uses similarity in SA results as a basis for organization, rather than similarity in physiographic  
334 characteristics. The derived regions are subsequently used to simplify model calibration across  
335 the CONUS and provide a basis for the transfer and application of parameters to ungaged areas.

336 The parameter sensitivities derived from the RR were used to organize the HRUs into two  
337 independently-derived calibration regions; the first derived by identifying HRUs with unique  
338 combinations of the order of parameter sensitivities to the RR (highest parameter sensitivities to  
339 lowest, i.e. 1-*Drofac* (78%), 2-*Rfactor* (16%), 3-*Meltcoef* (5%), 4-*Tsnow* (1%), 5-*Train* (1%)),  
340 and the second classification based upon identifying HRUs with unique sets of parameters whose  
341 sensitivities exceeded a specified threshold of parameter sensitivity (i.e. only *Drofac*, *Rfactor*,  
342 *Meltcoef* using a 5% threshold in the first classification example). The purpose of the first  
343 classification was to delineate regions of similar model response or behavior based on the order  
344 of importance of the MWBM parameters to the RR for each HRU. This classification identified  
345 16 distinct regions of HRUS across the CONUS based on the order of the parameter sensitivities  
346 of the five parameters (derived using the RR index). Sizes of these regions ranged from 94 km<sup>2</sup>  
347 to almost 2 million km<sup>2</sup>. The second classification delineated regions with an identical set of the  
348 most important parameters to the RR based on parameters whose sensitivities exceeded a 5%  
349 threshold. This step identified 12 regions of HRUs with unique combinations of parameter  
350 sensitivities exceeding 5%. There has been progress in providing quantitative thresholds for the  
351 identification of sensitive and non-sensitive parameters for hydrologic modelers (Tang et al.,  
352 2007), but no definitive consensus yet exists. Therefore a 5% threshold was used based on visual  
353 delineation of major physiographic features such as mountain ranges across the CONUS. The  
354 sizes of this second group of regions ranged from 94 km<sup>2</sup> to more than 15 million km<sup>2</sup>. Maps of  
355 the two groupings of HRUS were intersected to create a total of 49 regions across the CONUS.  
356 NHDPlus region and sub-region boundaries, proximity, and significant topographic divides were  
357 used to further divide the groups into 159 geographically unique calibration regions across the  
358 CONUS. The lack of streamgages available in some regions, especially areas with arid and  
359 semi-arid climates, necessitated merging regions together. Calibration regions that contained  
360 less than 3 streamgages from the 8,410 gages present in the Geospatial Fabric (see section 3.3)  
361 were combined with the proximate and most similar group which shared the most similar

362 parameter sensitivities (both order and magnitude), resulting in 110 calibration regions across  
363 the CONUS (Fig. 6). Within each region the FAST results for both the RR and RV indices were  
364 used to determine which parameters to calibrate. Within each region, parameters with a median  
365 parameter sensitivity of 5% for the RR and RV among the region's HRUs were selected for  
366 group calibration. Parameters not shown as sensitive were kept at the default value for the  
367 group.

368 *Figure 6. Final 110 Monthly Water Balance Model calibration regions differentiated by colors.*  
369 *A subset of streamgages within each calibration region were calibrated in a group-wise*  
370 *fashion to produce a single optimized parameter set for the entire region (Fig. 3).*

### 371 **3.3 Initial streamgage selection**

372 The initial set of streamgages used for testing in the MWBM calibration procedures was selected  
373 from 8,410 streamgages identified in the Geospatial Fabric (Fig. 7). The Geospatial Fabric  
374 includes reference and non-reference streamgages from the Geospatial Attributes of Gages for  
375 Evaluating Streamflow dataset (GAGES, Falcone et al., 2010). Of the 8,410 streamgages in the  
376 Geospatial Fabric, 1,864 were identified as having reference-quality data with at least 20 years of  
377 record. These reference quality streamgages were judged to be largely free of human alterations  
378 to flow (Falcone et al., 2010). In the current study, reference quality was not considered in the  
379 initial streamgage selection because the 20 years of record was considered too restrictive.  
380 Therefore a subset of the 8,410 streamgages was selected for initial testing in the MWBM  
381 calibration procedures based on the following criteria:

- 382 (1) Remove streamgages with less than 10 years of total measured streamflow (120 months)  
383 within the time period 1950 – 2010.
- 384 (2) Remove streamgages with a drainage area defined by the Geospatial Fabric that are not  
385 within 5% of the USGS National Water Information System (NWIS) reported drainage  
386 area (U.S. Geological Survey, 2014). This eliminated many of the streamgages with  
387 smaller drainage areas due to the resolution of the Geospatial Fabric.
- 388 (3) Remove streamgages that did not have at least 75% of its drainage area contained within  
389 a single calibration region.

390 These criteria resulted in 5,457 potential streamgages for testing in the MWBM calibration  
391 procedures (Fig. 7). Streamflow at these streamgages was aggregated and converted from daily  
392 (cubic feet/second) to a monthly runoff depth (mm) (streamflow per unit area).

393 *Figure 7. Streamgages tested in the study. GF notes geospatial fabric for national hydrologic*  
394 *modeling (Viger and Bock, 2014).*

### 395 **3.4 Monthly Water Balance Model calibration**

396 Two automated calibration procedures were implemented to produce an ‘optimal’ set of MWBM  
397 parameters for each calibration region. The first procedure, Individual Streamgage Calibration,  
398 calibrated each of the 5,457 streamgages individually. Results from the individual calibrations  
399 were used to further filter the streamgages within the second procedure, Grouped Streamgage  
400 Calibration, which calibrated selected streamgages together by calibration region.

#### 401 **3.4.1 Individual streamgage calibration**

402 The first calibration procedure was an automated process that individually calibrated each of the  
403 5,457 streamgages from the initial streamgage selection with measured streamflow (U.S.  
404 Geological Survey, 2014). Results from these individual streamgage calibrations quantified the  
405 ‘best’ performance of the MWBM at each gage, providing a ‘baseline’ measure for evaluation.

406 The Shuffled Complex Evolution (SCE) global-search optimization algorithm (Duan et al., 1993)  
407 has been frequently used as an optimization algorithm in hydrologic studies (Hay et al., 2006;  
408 Blasone et al. 2007; Arnold et al., 2012), including previous studies with the MWBM (Hay and  
409 McCabe, 2010). Further details can be found in Duan et al. (1993). SCE was used to maximize a  
410 combined objective function based on: (1) Nash-Sutcliffe Efficiency (NSE) coefficient using  
411 measured and simulated monthly runoff and (2) NSE using natural log-transformed measured  
412 and simulated runoff (logNSE), using the entire period of record for each streamgage. The NSE  
413 measures the predictive power of the MWBM in matching the magnitude and variability of the  
414 measured and simulated runoff (Nash and Sutcliffe, 1970). The NSE coefficient ranges from  $-\infty$   
415 to 1, with 1 indicating a perfect fit, and values less than 0 indicating that measured mean runoff  
416 is a better predictor than model simulations. The NSE has been shown to give more weight to  
417 the larger values in a time series (peak flows) at the expense of lower values (low flows)

418 (Legates and McCabe, 1999), so the logNSE was incorporated into the objective function to give  
419 weight to lowflow periods (Tekleab et al., 2011).

### 420 **3.4.2 Grouped streamgage calibration**

421 The second calibration procedure was an automated process that calibrated groups of  
422 streamgages together for each calibration region to derive a single set of MWBM parameters  
423 (Table 1) for each calibration region (Fig. 6). The NSE and logNSE values from the individual  
424 streamgage calibrations (described in the previous section) were used to identify streamgages  
425 that should not be used for grouped streamgage calibration. If the individual streamgage  
426 calibration was not ‘satisfactory’, then it was felt that it would not provide useful information for  
427 the grouped streamgage calibration procedure.

428 Satisfactory individual streamgage calibrations were identified with the following procedure:

- 429 (1) Eliminate all streamgages with NSE values  $< 0.3$ .
- 430 (2) If the number of remaining streamgages for a given calibration region is  $> 10$ , then  
431 eliminate all streamgages with NSE  $< 0.5$ .
- 432 (3) If the number of streamgages for a given calibration region is  $> 25$ , then eliminate all  
433 streamgages with  $NSE_{log} < 0$ .
- 434 (4) If the number of remaining streamgages for a calibration region is  $< 5$ , check to see if any  
435 of the eliminated streamgages were reference streamgages (as defined in Falcone et al, 2010),  
436 then add the reference streamgages back in if the NSE value  $> 0.0$ . Reference streamgages are  
437 USGS streamgages deemed to be largely free of anthropogenic impacts and flow modifications  
438 (Falcone et al., 2010; Kiang et al., 2013).

439 These criteria, while somewhat arbitrary, were chosen so that no calibration region had less than  
440 5 streamgages for the grouped streamgage calibration. Using the above criterion, of the 5,457  
441 streamgages individually calibrated, 3,125 remained as candidates for the grouped streamgage  
442 calibration procedure.



443 The grouped streamgauge calibration procedure used the SCE global-search optimization  
 444 algorithm with a multi-term objective function (Eq. 1). Measured and simulated values for  
 445 selected streamgages contained within a calibration region were scaled to Z-scores to remove  
 446 differences in magnitudes between streamgages (Eq. 2). The multi-term objective function  
 447 minimized the sum of the absolute differences between Z-scores from four measured and  
 448 simulated time series: mean monthly runoff (MMO, MMS), monthly runoff (MO, MS), annual  
 449 runoff (AO, AS) (U.S. Geological Survey, 2014), and monthly snow water equivalent (SO, SS))  
 450 for all selected streamgages within a given calibration region:

$$451 \quad \min \sum_{i=1}^n [3|MMO_i - MMS_i| + |MO_i - MS_i| + |AO_i - AS_i| + 0.5|SO_i - SS_i|] \quad (\text{Eq.1})$$

452

$$\text{where } \begin{cases} 0 & \text{if } 0.75 < SO_i - SS_i < 1.25 \\ |SO_i - SS_i| & \text{if } SS_i < SO_i^{0.75} \\ |SO_i - SS_i| & SS_i > SO_i^{1.25} \end{cases}$$

453 The measured and simulated Z-scores were calculated as:

$$454 \quad Z = (x-u)/\sigma \quad (\text{Eq. 2})$$

455 where x is the time-series value, u is the mean, and  $\sigma$  the standard deviation of the measured and  
 456 simulated variable.

457 ‘Measured’ SWE was determined for each HRU from the Snow Data Assimilation System  
 458 (SNODAS; National Operational Hydrologic Remote Sensing Center, 2004) and included a +/-  
 459 25% error bound. The unconstrained automated calibration (without a restriction on SWE) led to  
 460 unrealistic sources of snowmelt in the summer that enhanced the low-flow simulations. The 25%  
 461 error bound is arbitrary; calibrating to the actual SNODAS SWE values was found to be too  
 462 restrictive, but adding this error bound to the SWE values resulted in better overall runoff  
 463 simulations. The absolute difference of the simulated SWE Z-scores that were within +/- 25% of  
 464 the measured SWE Z-score were designated as 0. Otherwise, the absolute difference was  
 465 computed between the simulated SWE Z-score and either the upper or lower bounds (Eq. 1).

466 The grouped calibration procedure was run for all 110 calibration regions. For each calibration  
 467 region the seasonal adjustment parameters and the sensitive parameters (identified by the FAST

468 analysis -- section 3.1) were calibrated; parameters deemed not sensitive (parameter sensitivity <  
469 5% of total variance) were set to their default values (see Table 1). The entire period of the  
470 streamflow record for each streamgage was split by alternating years. After calibration, mean  
471 monthly measured and simulated Z-scores for runoff at all selected streamgages within a  
472 calibration region were compared.

473 Figure 8 shows an example of the graphic used to evaluate the measured and simulated mean  
474 monthly Z-scores for 21 streamgages selected for the region located in the Tennessee River  
475 calibration region (part of NHDPlus Region R06 in Fig. 2); the orange, red, and black dots  
476 indicate calibration, evaluation, and the entire period of record, respectively. A tight grouping  
477 around the one-to-one line indicates good correspondence between measured and simulated Z-  
478 scores. Points closer to the upper right corner of each plot represent high-flow periods. Points  
479 closer to the lower left corner of the plot represent low-flow periods. Streamgages within a  
480 calibration region were assigned the same parameter values; therefore streamgages that plotted  
481 outside (two standard deviations) of the one-to-one line were considered to not be representative  
482 of the calibration region, and the calibration procedure for that calibration region was repeated  
483 without those streamgages.

484 *Figure 8. Measured versus simulated mean monthly Z-scores for the Tennessee River*  
485 *calibration region (see Fig. 10b for location). Orange is calibration, red is evaluation, and*  
486 *black is all years.*

487 The goal of the second calibration procedure was to find a single parameter set for each  
488 calibration region. Past applications of the MWBM (Wolock and McCabe, 1999, McCabe and  
489 Wolock, 2011a) used a single set of fixed MWBM parameters for the entire CONUS. Many of  
490 the streamgages included in the second calibration procedure could be affected by significant  
491 anthropogenic effects; the seasonal adjustment factors, calibrated at each individual streamgage,  
492 could account for these effects and result in satisfactory NSE values. Streamgages that were  
493 removed due to poor performance in the second calibration were assumed to have anthropogenic  
494 effects not consistent with the streamgages that plotted along the one-to-one line. Poor  
495 performance may result because the MWBM fails to reliably simulate runoff for a watershed  
496 because of model limitations (i.e. not including all important hydrologic processes), but the

497 calibration regions are assumed to be homogeneous based on the FAST analysis. Therefore it is  
498 assumed that if some of the streamgages within a region have satisfactory results, then the  
499 MWBM is able to simulate runoff in that region.

## 500 **4 MWBM calibration region results**

### 501 **4.1 Individual streamgage calibration results**

502 The individual streamgage calibrations provided information regarding: (1) the potential  
503 suitability of a given streamgage for inclusion in a grouped calibration, and (2) a ‘baseline’  
504 measure for evaluation of the grouped calibration results. Reference and non-reference  
505 streamgages were considered in this application; if the runoff at a streamgage could not be  
506 calibrated individually to a ‘satisfactory’ level (based on criterion outlined in section 3.4.2), then  
507 it was felt that it would not provide useful information for the grouped streamgage calibration  
508 procedure. Figure 9 shows the NSE (Fig. 9a) and logNSE (Fig. 9b) coefficients from the  
509 individual streamgage calibrations for the CONUS. Scattered throughout the CONUS are NSE  
510 and logNSE values less than 0.0 (triangles in Fig. 9). These poor results are likely streamgages  
511 with poor streamflow records, either due to measurement error or anthropogenic effects (dams,  
512 water use, etc.).

513 *Figure 9. Individual streamgage calibration results: (a) Nash-Sutcliffe Efficiency (NSE)*  
514 *coefficient and (b) log of the NSE (logNSE).*

### 515 **4.2 Grouped streamgage calibration results**

#### 516 **4.2.1 Mean monthly z-scores**

517 Figure 10a shows a scatterplot of measured versus simulated mean monthly Z-scores for runoff,  
518 similar to Figure 8, but based on all available years (the black dots in Fig. 8) for all the final  
519 calibration streamgages (1,575 streamgages). Four regions are highlighted to illustrate the  
520 monthly variability in MWBM results across the CONUS (see Fig. 10b for locations). The four  
521 regions are: New England (67 streamgages, red); Tennessee River basin (21 streamgages,  
522 orange); Platte Headwaters (15 streamgages, blue); and Pacific Northwest (33 streamgages,  
523 green) (Fig. 10b).

524 *Figure 10. (a) Measured versus simulated mean monthly Z-scores for runoff at all streamgages*  
525 *and (b) location of highlighted streamgages for four calibration regions: New England (67*  
526 *streamgages, red); Tennessee River (21 streamgages, orange); Platte Headwaters (15*  
527 *streamgages, blue); and Pacific Northwest (33 streamgages, green).*

528 In Fig. 10a, three of the regions (New England, Tennessee River, and Pacific Northwest), show  
529 simulated Z-scores that correspond favorably to measured Z-scores for each of the twelve  
530 months, including periods of low and high runoff. These regions represent marine or humid  
531 climates with homogenous physio-climatic conditions and an even spatial distribution of  
532 streamgages, where models should be expected to perform well (see Fig. 9) There is a higher  
533 variability in model results for the high-flow months (May - June) for streamgages within the  
534 Platte Headwaters (Fig. 10a; blue dots) than for low-flow months. This variability may be  
535 related to factors controlling the magnitude and timing of snow melt runoff (Fig. 9).

536 For each calibration streamgage, a set of four months were identified that represent different  
537 parts of the measured mean monthly hydrograph (highest- and lowest- flow month and the two  
538 median-flow months). The measured and simulated mean monthly streamflow Z scores  
539 corresponding to the four months are plotted as cumulative frequencies (Fig. 11) to compare how  
540 well the simulated Z scores matched measured Z scores for different parts of the hydrograph  
541 over the entire set of calibration gages. For the highest-flow, there is an under-estimation of  
542 runoff, with the greatest divergence between the two distributions in the middle to lower half of  
543 the distribution (Fig. 11a). For the median-flow, the measured and simulated Z scores are well  
544 matched. For the 10 lowest-flow, simulated Z scores are greater than measured Z scores, with the  
545 greatest divergence between the two distributions in the middle to upper half of the distribution  
546 (Fig. 11c).

547 *Figure 11. Z-score cumulative frequency for (a) highest-, (b) median-, and (c) lowest-flow*  
548 *months.*

549 The median Z-score errors (simulated - measured) by region for the (a) highest-, (b) median-,  
550 and (c) lowest-flows are shown in Figure 12. The largest errors are for the highest-flows (Fig.  
551 12a). The MWBM simulations under-estimate the highest flows for much of the CONUS. The

552 errors for median-flows are fairly uniform and consistent across the CONUS (Fig. 12b), with a  
553 median error close to 0. For the lowest-flow months the MWBM over-estimates low flows for a  
554 large portion of the Midwest (Fig. 12c).

555 *Figure 12. Z-score error (simulated - measured) for (a) highest-, (b) median-, and (c) lowest-*  
556 *flow months.*

#### 557 **4.2.2 Nash-Sutcliffe efficiency**

558 Figure 13 compares the NSE from the individual streamgage calibrations (gageNSE) with the  
559 grouped calibrations (groupNSE) for all final streamgages used in the second calibration  
560 procedure. NSE values  $> 0.75$  (dashed line) and  $> 0.5$  (solid line) indicate very good and  
561 satisfactory results (Moriassi et al., 2007). Overall, most NSE values fall above the 0.5 NSE  
562 threshold of satisfactory performance (median of gageNSE and groupNSE = 0.76). The gageNSE  
563 values are used here as a ‘baseline’ for evaluation of the groupNSE results. The groupNSE  
564 values were not expected to be greater than the gageNSE values since (1) NSE was not used as  
565 an objective function in the grouped calibration, and (2) grouped calibrations found the ‘best’  
566 parameter set for a set of streamgages versus an individual streamgage. Figure 13 shows an equal  
567 distribution of NSE values around the one-to-one line, indicating that the grouped calibration  
568 provided additional information over the individual streamgage calibrations (cases where  
569 groupNSE are greater than gageNSE in Fig. 13). The difference between the gageNSE and  
570 groupNSE becomes larger as the NSE values decrease, reflecting the increasing uncertainty in  
571 the grouped calibrations in areas with lower gageNSE values.

572 *Figure 13. Nash Sutcliffe Efficiency from individual (gageNSE) and grouped (groupNSE)*  
573 *calibration. Calibration regions in New England (67 streamgages, red); Tennessee River*  
574 *(21 streamgages, orange); Platte Headwaters (15 streamgages, blue); and Pacific Northwest*  
575 *(33 streamgages, green) are highlighted (see Fig. 10b for location).*

576 Four regions are highlighted in Fig. 13 to illustrate the variability of NSE across the CONUS  
577 (see Fig. 10b for locations). The highlighted regions in New England (red), Tennessee River  
578 (orange), and Pacific Northwest (green), show good groupNSE and gageNSE results. Four of

579 the 15 streamgages in the Platte Headwaters (blue) have groupNSE values  $\leq 0.5$ . This is  
580 probably related to simulation error during the snowmelt period (May - June, Fig. 10a).

581 Figure 14 shows the median groupNSE by calibration region for the CONUS. The pattern is very  
582 similar to that shown for the individual streamgage calibration results in Fig. 9a and highlights  
583 the problem areas shown in Fig. 12.

584 *Figure 14. Median Nash Sutcliffe Efficiency (NSE) of streamgages used for calibration by*  
585 *calibration region.*

586

## 587 **5 Discussion**

588 This study presented a parameter regionalization procedure for calibration of the MWBM,  
589 resulting in an application that can be used for simulation of hydrologic variables for both gaged  
590 and ungaged areas in the CONUS. The regionalization procedure grouped HRUs on the basis of  
591 similar sensitivity to five model parameters. Parameter values and model uncertainty  
592 information within a group was then passed from gaged to ungaged areas within that group.

### 593 **5.1 Regionalized parameters**

594 Results from this study indicate that regionalized parameters can be used to produce satisfactory  
595 MWBM simulations in most parts of the CONUS (Fig. 13). Despite the differences between the  
596 individual streamgage calibration and grouped calibration, Figure 13 illustrates that the grouped  
597 calibration strategy, which focused only on sensitive parameters, can provide just as much  
598 information as the individual streamgage calibration with no constraints on the parameter  
599 optimization other than the default ranges. The MWBM is a simple hydrologic model as it has  
600 minimal parameters, which are conceptual in nature (not physically based). It may be that this  
601 type of model is best for regionalization when parameter sensitivity can be identified and HRU  
602 behavior can be classified by a small number of clearly defined spatial groups. More  
603 complicated models with many more interactive parameters may not respond as well to this  
604 simple type of regionalization; more parameters may lead to more parameter interaction and  
605 situations of equifinality which might confuse the analysis.

606 The adjustments of precipitation and temperature parameters for the individual streamgage  
607 calibrations accounted for local errors such as rain gage under catch of precipitation. In addition  
608 these climate adjustments also account for local anthropogenic effects on streamflow (e.g. dams,  
609 diversions) since streamgages were not screened for these effects prior to individual streamgage  
610 calibration. In the grouped streamgage calibrations, the same precipitation and temperature  
611 adjustments are applied at every streamgage within the calibration region, making these climate  
612 adjustments more of a regional adjustment and producing more of a ‘reference’ condition for  
613 each calibration region.

## 614 **5.2 Parameter sensitivities and dominant process**

615 The MWBM parameter sensitivities varied by hydroclimatic index (RR and RV) and across the  
616 CONUS (Fig. 3). The parameter sensitivity patterns give an indication of dominant hydrologic  
617 processes based on MWBM. The dominant process can be seasonal and MWBM performance  
618 may be enhanced by extending the use of SA along the temporal domain to identify and  
619 temporally vary the parameters that are seasonally important to the MWBM. For example, error  
620 in peak flow months is the primary cause for poor model performance in the Platte Headwaters  
621 (Fig. 9). For the Platte Headwaters, the final parameter set performed well for simulated Z-  
622 scores for the regionalized low- and median-flow conditions (Fig. 9a, July through April), but  
623 was not able to replicate measured mean monthly flows for May and June. In this case, the  
624 dominant processes controlling hydrologic behavior change with season and the parameters  
625 controlling the dominant response may have to change accordingly (Gupta et al., 2008; Reusser  
626 et al., 2011).

## 627 **5.3 Model accuracy**

628 The pattern of MWBM accuracies shown in Fig. 8 and 14 are similar to those shown by Newman  
629 et al. (2015; Fig. 5a) in which a daily time-step hydrologic model was calibrated for 671 basins  
630 across the CONUS. Our study and the Newman et al. (2015) study both indicate the same  
631 ‘problem areas’ with the poorest performing basins generally being located in the high plains and  
632 desert southwest. Newman et al. (2015) attributed variation in model performance by region to

633 spatial variations in aridity and precipitation intermittency, contribution of snowmelt, and runoff  
634 seasonality.

635 The inferior MWBM results in the ‘problem areas’ can be attributed to multiple factors which  
636 likely include inadequate hydrologic process representation and errors in forcing data (e.g.  
637 climate data), and/or measured streamflow. Archfield et al. (2015) state that the performance of  
638 continental-domain hydrologic models is considerably constrained by inadequate model  
639 representation of dominant hydrologic processes. For example, the simplicity of the MWBM  
640 presents limitations on the representation of deeper groundwater reservoirs, gaining and losing  
641 stream reaches, simplistic AET, and the effects of surface processes (infiltration and overland  
642 flow) that need to be represented at finer time steps than monthly.

643 The dominant hydrologic processes in the ‘problem areas’ appear to be poorly represented at the  
644 daily (Newman et al., 2015) and monthly time steps. This may be due to inadequate forcing  
645 data, the quality of which ‘is paramount in hydrologic modeling efforts’ (Archfield et al., 2015)  
646 and/or the lack of ‘good’ reference streamflow data for calibration and evaluation. Both surely  
647 play a role and emphasize the need for incorporation of additional datasets so that calibration and  
648 evaluation of intermediate states in the hydrologic cycle are examined.

## 649 **6 Conclusions**

650 A parameter regionalization procedure was developed for the CONUS that transferred parameter  
651 values from gaged to ungaged areas for a MWBM. The FAST global-sensitivity algorithm was  
652 implemented on a MWBM to generate parameter sensitivities on a set of 109,951 HRUs across  
653 the CONUS. The parameter sensitivities were used to group the HRUs into 110 calibration  
654 regions. Streamgages within each calibration region were used to calibrate the MWBM  
655 parameters to produce a regionalized set of parameters for each calibration region. The  
656 regionalized MWBM parameter sets were used to simulate monthly runoff for the entire  
657 CONUS. Results from this study indicate that regionalized parameters can be used to produce  
658 satisfactory MWBM simulations in most parts of the CONUS.

659 The best MWBM results were achieved simulating low- and median-flows across the CONUS.  
660 The high-flow months generally showed lower skill levels than the low- and median-flow



661 months, especially for regions with dominant seasonal cycles. The lowest MWBM skill levels  
662 were found in the high plains and desert southwest and can be attributed to multiple factors  
663 which likely include inadequate hydrologic process representation and errors in forcing data  
664 and/or measured streamflow. Calibration and evaluation of intermediary fluxes and states in the  
665 MWBM through additional measured datasets may help to improve MWBM representations of  
666 these model states by helping to constrain parameterization to measured values.

667 **7 Acknowledgments**

668 This research was financially supported by the U.S. Department of Interior South Central  
669 Climate Science Center (<http://southcentralclimate.org/>), U.S. Environmental Protection Agency  
670 Office of Water, and the U.S. Geological Survey WaterSMART initiative. This paper is a  
671 product of discussions and activities that took place at the USGS John Wesley Powell Center for  
672 Analysis and Synthesis (<https://powellcenter.usgs.gov/>). Further project support was provided  
673 by the Jeff Falgout of the USGS Core Science Systems (CSS) Mission Area. Any use of trade,  
674 product, or firm names is for descriptive purposes only and does not imply endorsement by the  
675 U.S. Government.

676

677

678

679

680

681

682

683

684

685

686

687

688 **8 References**

689 Adam, J.C., and Lettenmaier, D.P.: Bias correction of global gridded precipitation for solid  
690 precipitation undercatch, *J. Geophys. Res.*, 108, 1-14, doi:10.1029/2002JD002499, 2003.

691 Ali, G., Tetzlaff, D., Soulsby, C., McDonnell, J.J., and Capell, R.: A comparison of similarity  
692 indices for catchment classification using a cross-regional dataset, *Adv. Water Resources*, 40,  
693 11-22, <http://dx.doi.org/10.1016/j.advwatres.2012.01.008>, 2012.

694 Archfield, S.A., Clark, M., Arheimer, B., Hay, L.E., Farmer, W.H, McMillan, H., Seibert, J.,  
695 Kiang, J.E., Wagener, T., Bock, A., Hakala, K., Andressian, V., Attinger, S., Viglione, A.,  
696 Knight, R.R., and Over, T.: Accelerating advances in continental domain hydrologic modeling,  
697 *Water Resour. Res.*, 51, 10078-10091, doi: 10.1002/2015WR017498, 2015.

Comment [Bock4]: Finalized reference

698 Arnold, J.G., Moriasi, D.N., Gassman, P.W., Abbaspour, K.C., White, M.J., Srinivasan, R.,  
699 Santhi, C., Harmel, R.D., van Griensven, A., Van Liew, M.W., Kannan, N., and Jha, M.K.:  
700 SWAT: Model Use, Calibration and Validation, *T. ASABE*, 55(4), 1491-1508, doi:  
701 10.13031/2013.42256, 2012.

702 Blasone, R.S., Madsen, H., and Rosbjerg, D.: Parameter estimation in distributed hydrological  
703 modelling: comparison of global and local optimisation techniques, *Nord. Hydrol.*, 34,451-476,  
704 doi:10.2166/nh.2007.024, 2007.

705 Blodgett, D.L., Booth, N.L., Kunicki, T.C., Walker, J.L., and Viger, R.J.: Description and  
706 Testing of the Geo Data Portal: A Data Integration Framework and Web Processing Services for  
707 Environmental Science Collaboration. US Geological Survey, Open-File Report 2011-1157, 9  
708 pp., Middleton, WI, USA, 2011.

709 Blöschl, G., and Sivapalan, M.: Scale issues in hydrological modeling: a review, *Hydrol.*  
710 *Process.*, 9, 251-290, doi:10.1002/hyp.3360090305, 1995.

711 Blöschl, G., Sivapalan, M., Wagener, T., Viglione, A., and Savenije, H (Eds.): *Runoff*  
712 *Prediction in Ungauged Basins: Synthesis across Processes, Places, and Scales*. Cambridge  
713 University Press, Cambridge, England, 2013.

714 Clark, M.P., and Slater, A.G.: Probabilistic Quantitative Precipitation Estimation in Complex  
715 Terrain, B. Am. Meteorol. Soc., 7, 3-2, doi: <http://dx.doi.org/10.1175/JHM474.1>, 2006.

716 Cukier, R.I., Fortuin, C.M., Shuler, K.E., Petschek, A.G, and Schaibly, J.H: Study of sensitivity  
717 of coupled reaction systems to uncertainties in rate coefficients 1, J. Chem. Phys., 59(8), 3873-  
718 3878, doi:10.1063/1.1680571, 1973.

719 Cukier, R.I., Schiably, J.H., and Shuler, K.E: Study of sensitivity of coupled reaction systems to  
720 uncertainties in rate coefficients 3, J. Chem. Phys., 63(3), 1140-1149, doi:1063/1.431440, 1975.

721 Cuo, L., Giambelluca, T.W., and Ziegler, A.D: Lumped parameter sensitivity analysis of a  
722 distributed hydrological model within tropical and temperate catchments, Hydrol. Process.,  
723 25(15), 2405-2421, doi:10.1002/hyp.8017, 2011.

724 Duan, Q., Gupta, V.K., and Sorooshian, S.: A shuffled complex evolution approach for effective  
725 and efficient optimization, J. Optimiz. Theory App., 76, 501-521, doi:10.1007/BF00939380,  
726 1993.

727 Falcone, J.A., Carlisle, D.M., Wolock, D.M., and Meador, M.R.: GAGES: A stream gage  
728 database for evaluating natural and altered flow conditions in the conterminous United States,  
729 Ecology, 91, p. 621, A data paper in Ecological Archives E091-045-D1, available at  
730 <http://esapubs.org/Archive/ecol/E091/045/metadata.htm> (last accessed 15 November 2012),  
731 2010.

732 Farnsworth, R.K., Thompson, E.S., and Peck, E.L.: Evaporation Atlas for the Contiguous 48  
733 United States, NOAA Technical Report NWS 33, 41 pp., National Oceanic and Atmospheric  
734 Administration, Washington, D.C., 1982.

735 Groisman, P.Y., and Legates, D.R.: The accuracy of United States precipitation data, Bull. Am.  
736 Meteorol. Soc., 75(2), 215-227, doi: 10.1175/1520-0477(1994)075<0215:TAOUSP>2.0.CO;2,  
737 1994.

Comment [Bock5]: Added doi number

Comment [Bock6]: Added doi number

738 Gupta, H.V., Wagener, T., Liu, Y.Q. "Reconciling theory with observations: Elements of  
739 diagnostic approach to model evaluation," Hydrologic Processes (2008), 22, 3802-3813, doi:  
740 10.1002/hyp.6989, 2008.

741 Guse, B., Reusser, D.E., and Fohrer, N.: How to improve the representation of hydrological  
742 processes in SWAT for a lowland catchment - temporal analysis of parameter sensitivity and  
743 model performance, Hydrol. Process., 28(4), 2561-2670, doi:10.1002/hyp.9777, 2013.

744 Hay, L.E., Leavesley, G.H., Clark, M.P., Markstrom, S.L., Viger, R.J., and Umemoto, M.: Step-  
745 wise multiple-objective calibration of a hydrologic model for a snowmelt-dominated basin, J.  
746 Am. Water Resour. A., 42(4), 877-890, doi:10.1111/j.1752-1688.2006.tb04501.x, 2006.

747 Hay, L.E., and McCabe, G.J.: Spatial Variability in Water-Balance Model Performance in the  
748 Conterminous United States, J. Am. Water Resour. Assoc., 38(3), 847-860, DOI:  
749 10.1111/j.1752-1688.2002.tb01001.x, 2002.

750 Hay, L.E., and McCabe, G.J.: Hydrologic effects of climate change in the Yukon River Basin,  
751 Climate Change, 100, 509-523, doi:10.1007/s10584-010-9805-x, 2010.

752 Kapangaziwiri, E., Hughes, D. A., and Wagener, T.: Constraining uncertainty in hydrological  
753 predictions for ungauged basins in southern Africa, Hydrol. Sci. J., 57, 1000–1019, 5  
754 doi:10.1080/02626667.2012.690881, 2012.

755 Kiang, J.E., Stewart, D.W., Archfield, S.A., Osborne, E.B., and Eng, K.: A National Streamflow  
756 Network Gap Analysis. U.S. Geological Survey, Scientific Investigative Reports 2013-5013, 94  
757 pp., Reston, VA, USA, 2013.

758 Kirchner, J.W.: Getting the right answers for the right reasons: Linking measurements,  
759 analyses, and models to advance the science of hydrology, J. Hydrol., 42, W03S04,  
760 doi:10.1029/2005WR004362, 2006.

761 Kokkonen, T.S., Jakeman, A.J., Young, P.C., and Koivusalo, H.J.: Predicting daily flows in  
762 ungauged catchments: model regionalization from catchment descriptors at the Coweeta

**Comment [Bock7]:** Incorrectly formatted reference, added doi number

763 Hydrologic Laboratory, North Carolina, Hydrol. Process., 17, 2219-2238, doi:10.1002/hyp.1329,  
764 2003.

765 Krause, P., Doyle, D. P., and Bäse, F.: Comparison of different efficiency criteria for  
766 hydrological model assessment, Adv. Geosci., 5, 89–97, doi:10.5194/adgeo-5-89-2005, 2005.

767 Legates, D.R., and McCabe,G.J.: Evaluating the use of “goodness-of-fit” Measures in  
768 hydrologic and hydroclimatic model validation, Water Resour. Res., 35(1), 233-241,  
769 doi:10.1029/1998WR900018, 1999.

770 Maurer, E.P., Wood, A.W., Adam, J.C., Lettenmaier, D.P., and Nijseen, B.: A long-term  
771 hydrologically-based data set of land surface fluxes and states for the conterminous United  
772 States, J. Climatol., 15, 3237-3251, [http://dx.doi.org/10.1175/1520-](http://dx.doi.org/10.1175/1520-0442(2002)015<3237:ALTHBD>2.0.CO;2)  
773 [0442\(2002\)015<3237:ALTHBD>2.0.CO;2](http://dx.doi.org/10.1175/1520-0442(2002)015<3237:ALTHBD>2.0.CO;2), 2002.

774 McCabe, G.J., Hay, L.E., Bock, A., Markstrom, S.L., and Atkinson, R.D.: Inter-annual and  
775 spatial variability of Hamon potential evapotranspiration model coefficients, J. Hydrol., 521,  
776 389-394, doi:10.1016/j.jhydrol.2014.12.006, 2015.

777 McCabe, G.J., and Markstrom, S.L.: A Monthly Water-Balance Model Driven By a Graphical  
778 User Interface. U.S. Geological Survey Open-File Report 2007-1008, 12 pp., Reston, VA, USA,  
779 2007.

780 McCabe, G.J., and Wolock, D.M.: Century-scale variability in global annual runoff examined  
781 using a water balance model, Int. J. Clintol., 31, 1739-1748, doi:10.1002/joc.2198, 2011a.

782 McCabe, G.J., and Wolock, D.M.: Independent effects of temperature and precipitation on  
783 modeled runoff in the conterminous United States, Water Resour. Res., 47, W1152,  
784 doi:10.1029/2011WR010630, 2011b.

785 McManamay, R.A., Orth, D.J., Dolloff, C.A., and Frimpong, E.A: Regional Frameworks  
786 applied to Hydrology: Can Landsapes-based frameworks capture the hydrologic variability?,  
787 River Res. App., 28, 1325-1339, doi:10.1002/rra.1535, 2011.

788 Merz, R., and Blöschl, G.: Regionalisation of catchment model parameters, *J. Hydrol.*, 287, 95-  
789 123, doi:10.1016/j.jhydrol.2003.09.028, 2004.

790 Moriasi, D.N, Arnold, J.G., Van Liew, M.W., Bingner, R.L., Harmel, R.D., and Vieth, T.L.:  
791 Model Evaluation Guidelines for Systematic Quantification of Accuracy in Watershed  
792 Simulations, *T. ASABE*, 50, 885-900, doi: 10.13031/2013.23153, 2007.

793 Nash, J.E., and Sutcliffe, J.V.: River flow forecasting through conceptual models Part I: a  
794 discussion of principles, *J. Hydrol.*, 10, 282-290, doi:10.1016/0022-1694(70)90255-6, 1970.

795 National Operational Hydrologic Remote Sensing Center, Snow data Assimilation System  
796 (SNODAS) Data Products at the NSIDC, 9/30/2003 through 6/13/2014, National Snow and Ice  
797 Data Center, Boulder, Colorado, USA, <http://dx.doi.org/10.7265/N5TB14TC>, 2004.

798 Newman, A.J., Clark, M.P., Sampson, K., Wood, A., Hay, L.E., Bock, A., Viger, R.J., Blodgett,  
799 D., Brekke, L., Arnold, J.R., Hopson, T., and Duan, Q.: Development of a large-sample  
800 watershed-scale hydrometeorological data set for the contiguous USA: data set characteristics  
801 and assessment of regional variability in hydrologic model performance, *Hydrol. Earth Syst. Sc.*,  
802 19, 209-223, doi:10.5194/hess-19-209-2015, 2015.

803 Oudin, L., Andréassian, V., Perrin, C., Michel, C., and Le Moine, N.: Spatial proximity,  
804 physical similarity, regression and ungaged catchments: a comparison of regionalization  
805 approaches based on 913 French catchments, *Water Resour. Res.*, 44, 1-15,  
806 doi:10.1029/2007WR006240, 2008.

807 Oudin, L., Kay, A., Andréassian, V., and Perrin, C.: Are seemingly physically similar  
808 catchments truly hydrologically similar?, *Water Resour. Res.*, 46, W11558,  
809 doi:10.1029/2009WR008887, 2010.

810 Oyler, J.W., Dobrowski, S.Z., Ballantyne, A.P., Klene, A.E., and Running, S.W.: Artificial  
811 amplification of warming trends across the mountains of the western United States, *Geophys.*  
812 *Res. Lett.*, 42, 153-161, doi:10.1002/2014GL062803, 2015.

813 Peel, M.C., Chiew, F.H.S., Western, A.W., and McMahon, T.A.: Extension of unimpaired  
814 monthly streamflow data and regionalization of parameter values to estimate streamflow in  
815 ungauged catchments. Report to National Land and Water Resources Audit, Center for  
816 Environmental Application and Hydrology, University of Melbourne, Parkville, 2000.

817 R Core Team: R: A language and environment for statistical computing, R Foundation for  
818 Statistical Computing, Vienna, Austria, 2013.

819 Reusser, D.: fast: Implementation of the Fourier Amplitude Sensitivity Test (FAST), R package  
820 version, <http://CRAN.R-project.org/package=fast>, (last access: 9 April 2014), 2012.

821 Reusser, D., Buytaert, W., and Zehe, E.: Temporal dynamics of model parameter sensitivity for  
822 computationally expensive models with the Fourier amplitude sensitivity test, *Water Resour.*  
823 *Res.*, 47, W07551, doi:10.1029/2010WR009947, 2011.

824 Saltelli, A., Tarantola, S., and Campolongo, F.: Sensitivity analysis as an ingredient of  
825 modeling, *Stat. Sci.*, 15, 377-395, 2000.

826 Samuel, J., Coulibaly, P., and Metcalfe, R.A.: Estimation of Continuous Streamflow in Ontario  
827 Ungauged Basins: Comparison of Regionalization Methods, *J. Hydrol. Eng.*, 16, 447-459,  
828 [http://dx.doi.org/10.1061/\(ASCE\)HE.1943-5584.0000338](http://dx.doi.org/10.1061/(ASCE)HE.1943-5584.0000338), 2011.

829 Sankarasubramanian, A., and Vogel, R.M.: Hydroclimatology of the continental United States,  
830 *Geophys. Res. Lett.*, 30, 1-4, doi:10.1029/2002GL015937, 2003.

831 Santhi, C., Kannan, N., Arnold, J.G., and Diluzio, M.: Spatial calibration and temporal  
832 validation of flow for regional scale hydrologic modeling, *J. Am. Water Resour. Assoc.*, 4, 829-  
833 846, doi:10.1111/j.1752-1688.2008.00207.x, 2008.

834 Sawicz, K., Wagener, T., Sivapalan, M., Troch, P.A., and Carrillo, G.: Catchment classification:  
835 empirical analysis of hydrologic similarity based on catchment function in the eastern USA,  
836 *Hydrol. Earth Syst. Sc.*, 15, 2895-2911, doi:10.5194/hess-15-2895-2011, 2011.



837 Sefton, C.E.M., and Howarth, S.M.: Relationships between dynamic response characteristics  
838 and physical descriptors of catchments in England and Wales, *J. Hydrol.*, 211, 11-16,  
839 doi:10.1016/S0022-1694(98)00163-2, 1998.

840 Seibert, J.: Regionalization of parameters for a conceptual rainfall runoff model, *Agr. Forest*  
841 *Meteorol.*, 98-99, 279-293, doi:10.1016/S0168-1923(99)00105-7, 1999.

842 Smakhtin, V.U.: Low flow hydrology: a review, *J. Hydrol.*, 240, 147-186, doi:10.1016/S0022-  
843 1694(00)00340-1, 2001.

844 Tang, Y., Reed, P., Wagener, T., and van Werkhoven, T.: Comparing sensitivity analysis  
845 methods to advance lumped watershed model identification and evaluation, *Hydrol. Earth Syst.*  
846 *Sci.*, 11, 793-817, doi: 10.5194/hess-11-793-2007, 2007.

847 Tekleab, S., Uhlenbrook, S., Mohamed, Y., Savenije, H.H.G., Temesgen, M., and Wenninger, J.:  
848 Water balance modeling of Upper Blue Nile catchments using a top-down approach, *Hydrol.*  
849 *Earth Syst. Sci.*, 15, 2179-2193, doi:10.5194/hess-15-2179-2011, 2011.

850 Troch, P.A., Paniconi, C., and McLaughlin, D.: Catchment-scale hydrological modeling and  
851 data assimilation, *Adv. Water Resour.*, 26, 131-135, doi:10.1016/S0309-1708(02)00087-8, 2003.

852 US Geological Survey: A National Water Information System, available at: <http://waterdata.usgs.gov/nwis/> (last access 27 March 2014), 2014.

854 US Environmental Protection Agency and US Geological Survey: NHDPlus User guide,  
855 available at: [ftp://ftp.horizon-systems.com/NHDPlus/documentation/NHDPLUS\\_UserGuide.pdf](ftp://ftp.horizon-systems.com/NHDPlus/documentation/NHDPLUS_UserGuide.pdf)  
856 (last access November 2014), 2010.

857 van Griensven, A., Meixner, T., Grunwald, S., Bishop, T., Diluzio, and M., Srinivasan, R.: A  
858 global sensitivity analysis tool for the parameters of multi-variable catchment models, *J. Hydrol.*,  
859 324, 10-23, doi:10.1016/j.jhydrol.2005.09.008, 2006.

Comment [Bock8]: Added reference for NHDPlus

860 Vandewiele, G.L., and Elias, A.: Monthly water balance of ungaged catchments obtained by  
861 geographical regionalization, *J. Hydrol.*, 170, 277-291, doi:10.1016/0022-1694(95)02681-E,  
862 1995.

863 Viger, R., and Bock, A.: GIS Features of the Geospatial Fabric for National Hydrologic  
864 Modeling, U.S. Geological Survey, Denver, CO, USA, doi:10.5066/F7542KMD, 2014.

865 Vogel, R.M.: Regional calibration of watershed models, *Watershed Models*, Singh, V.P., and  
866 Frevert, D.F. (Eds.), CRC Press, Boca Raton, FL, USA, 2006.

867 Vrugt, J.A., ter Braak, C.J.F., Clark, M.P., Hyman, J.M., and Robinson, B.A.: Treatment of  
868 input uncertainty in hydrologic modeling: Doing hydrology backwards with Markov Chain  
869 Monte Carlo simulation, *Water Resour. Res.*, 44, W00B09, doi:10.1029/2007WR006720, 2008.

870 Wolock, D.M.: STATSGO soil characteristics for the conterminous United States. U.S.  
871 Geological Survey Open-File Report 1997-656, Reston, VA, USA, available at:  
872 <http://water.usgs.gov/GIS/metadata/usgswrd/XML/muid.xml>, (last access 3 March 2012), 1997.

873 Wolock, D.M., and McCabe, G.J.: Explaining spatial variability in mean annual runoff in the  
874 conterminous United States, *Clim. Res.*, 11, 149-159, doi:10.3354/cr011149, 1999.

875 Zhang, X., Srinivasan, R., and Van Liew, M.: Multi-Site Calibration of the SWAT Model for  
876 Hydrologic Modeling, *T. ASABE*, 51, 2039-2049, doi:10.13031/2013.25407, 2008.

877

878

879

880

881

882

883

884

885

886

887

888

<b>Parameter</b>	<b>Definition</b>	<b>Range</b>	<b>Default</b>
<b>1. <i>Drofac</i></b>	Controls fraction of precipitation that becomes runoff	0, 0.10	0.05
<b>2. <i>Rfactor</i></b>	Controls fraction of surplus that becomes runoff	0.10, 1.0	0.5
<b>3. <i>Tsnow</i></b>	Threshold above which all precipitation is rain (°C)	-10.0, -2.0	-4.0
<b>4. <i>Train</i></b>	Threshold below which all precipitation is snow (°C)	0.0, 10.0	7.0
<b>5. <i>Meltcoef</i></b>	Proportion of snowpack that becomes runoff	0.0, 1.0	0.47
<b>6. <i>Ppt_adj</i></b>	Seasonal adjustment factor for precipitation (%)	0.5, 2.0	1
<b>7. <i>Tav_adj</i></b>	Seasonal adjustment for temperature (°C)	-3.0,3.0	0

889

890

Table 1. Monthly Water Balance Model parameters and ranges.

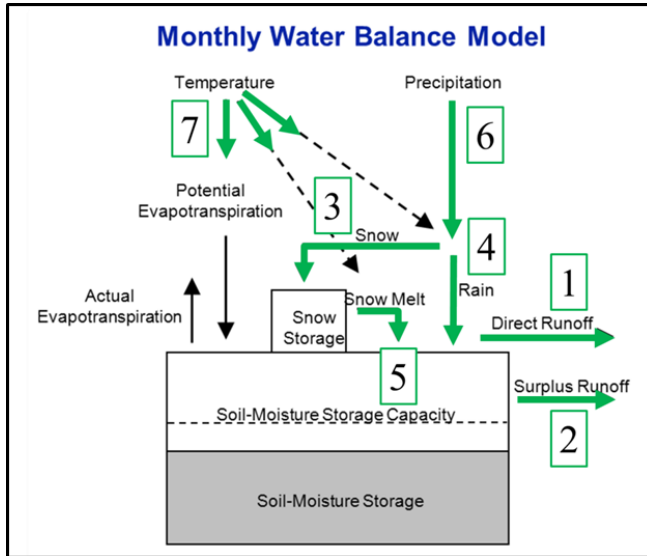
891

892

893

894

895



896

897 Figure 1. Conceptual diagram of the Monthly Water Balance Model (McCabe and Markstrom  
898 2007). Processes influenced by model parameters used in Fourier Amplitude Sensitivity Test  
899 (FAST) those identified by green arrow and numbered 1-5 (Table 1).

900

901

902

903

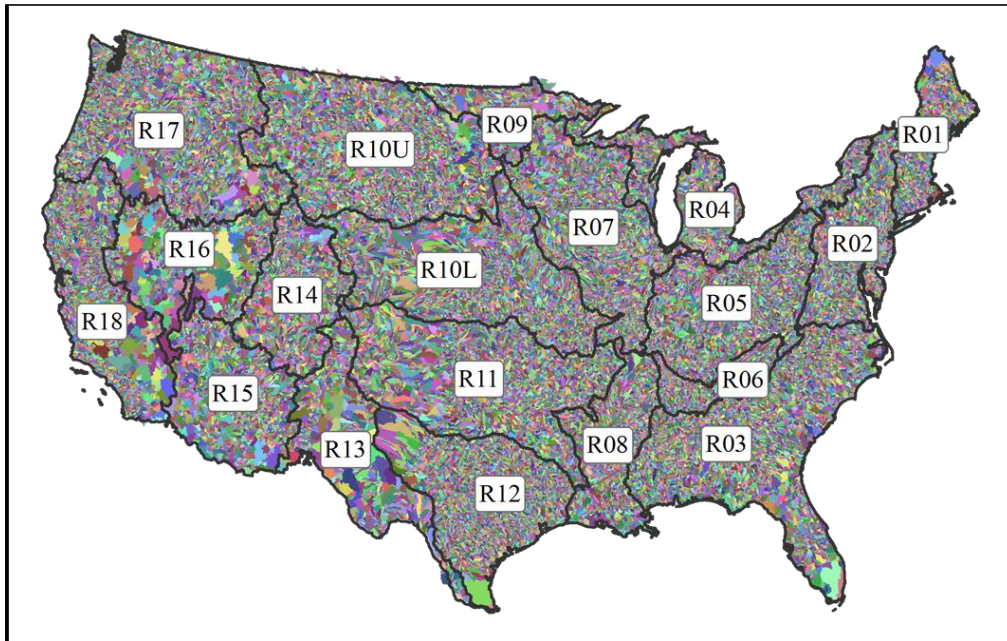
904

905

906

907

908



909

910 Figure 2. Hydrologic Response Units of the Geospatial Fabric, differentiated by color, overlain  
911 by NHDPlus region boundaries (R01-R18).

912

913

914

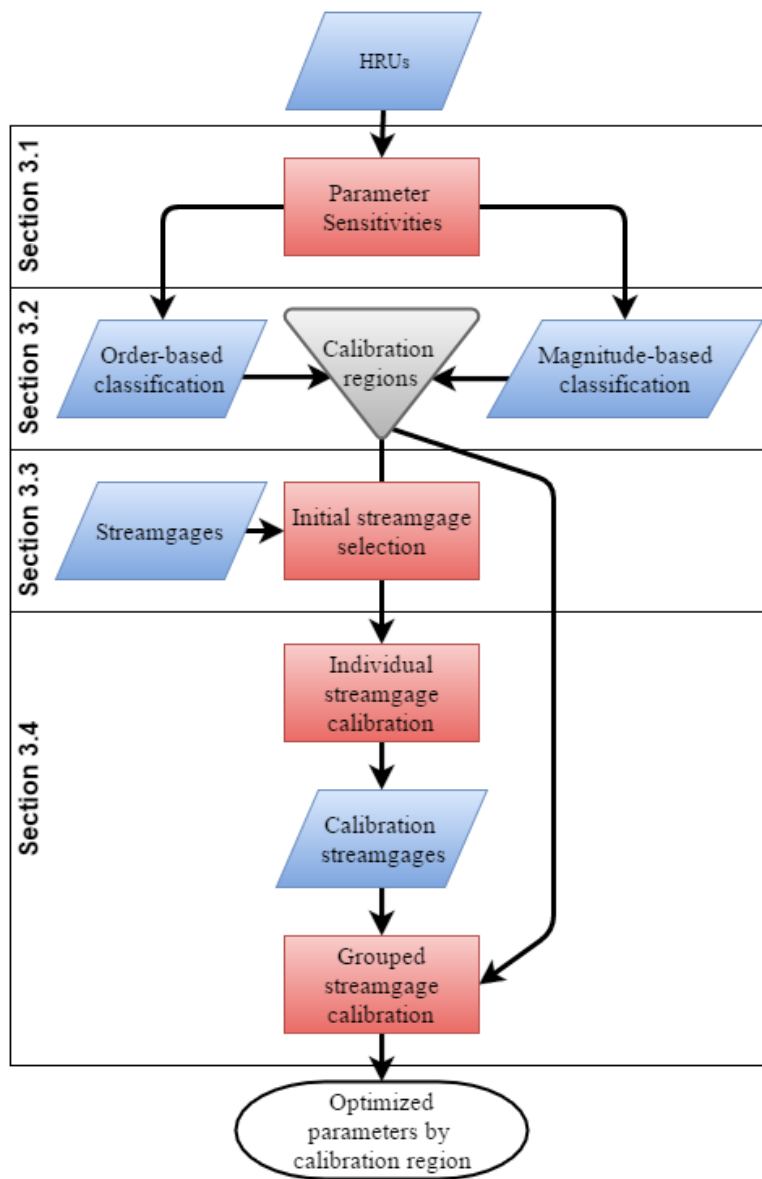
915

916

917

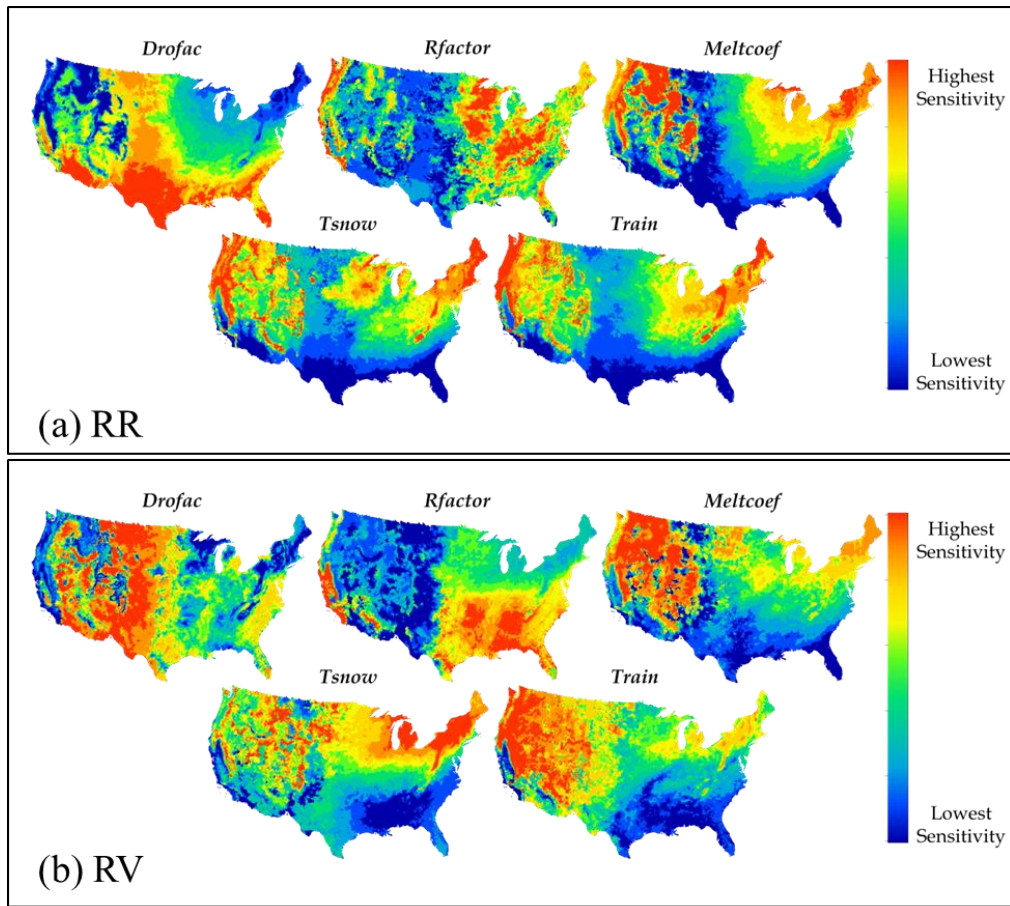
918

919



920

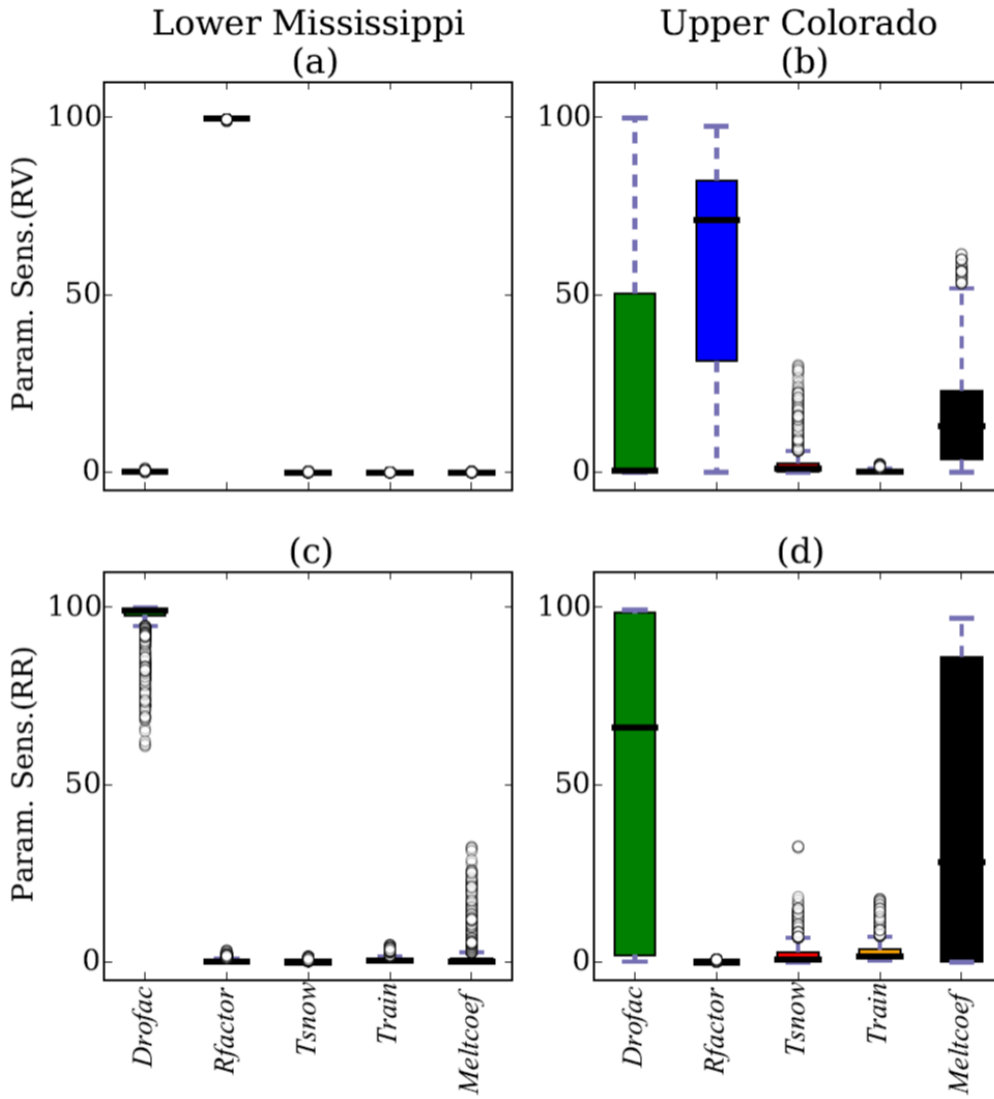
921 Figure 3. Schematic flowchart of the parameter regionalization procedure described in Section  
922 3: Parameter sensitivities (3.1), Calibration regions (3.2), Initial streamgauge selection (3.3), and  
923 Grouped streamgauge calibration (3.4).



924  
925 Figure 4. Relative sensitivity of the (a) Rainfall Ratio (RR) and (b) Runoff Variability (RV)  
926 indices to Monthly Water Balance Model parameters.

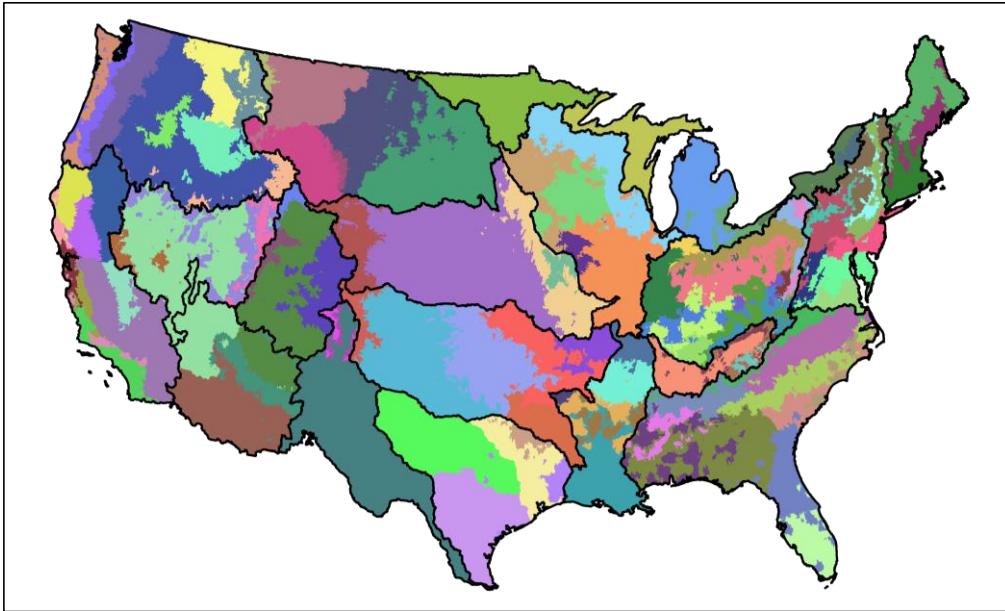
927

928



930 Figure 5. Parameter sensitivities of Runoff Variability (RV; a and b) and Runoff Ratio (RR; c  
 931 and d) indices for Monthly Water Balance Model parameters in the Lower Mississippi (R08) and  
 932 Upper Colorado (R14).  
 933





935

936 Figure 6. Final 110 Monthly Water Balance Model calibration regions differentiated by colors.  
937 A subset of streamgages within each calibration region were calibrated in a group-wise fashion  
938 to produce a single optimized parameter set for the entire region (Fig. 3).

939

940

941

942

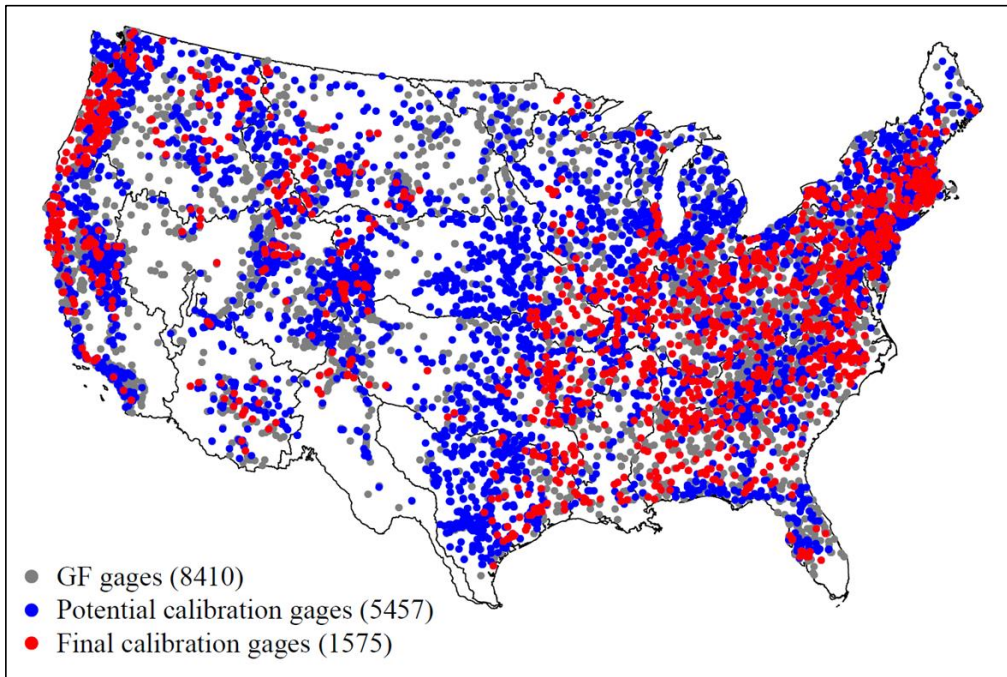
943

944

945

946

947



948

949 Figure 7. Streamgages tested in the study. GF notes geospatial fabric for national hydrologic  
950 modeling (Viger and Bock, 2014).

951

952

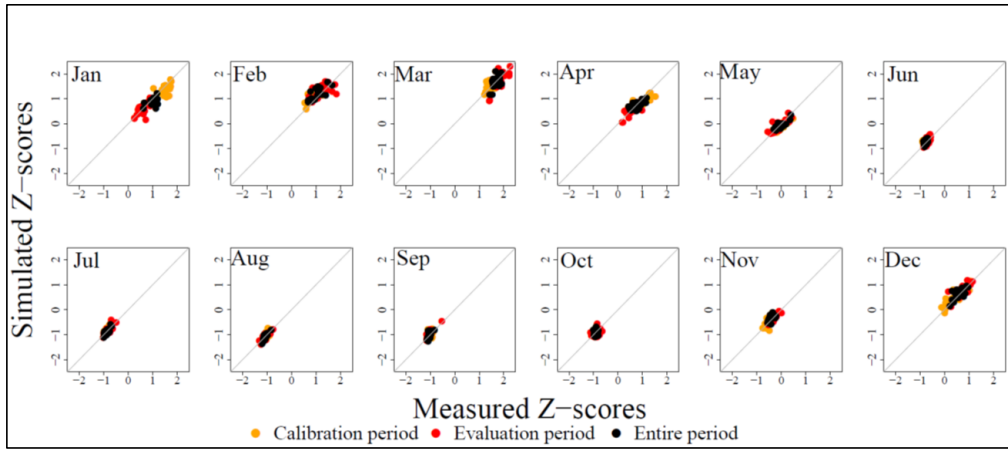
953

954

955

956

957



958

959 Figure 8. Measured versus simulated mean monthly Z-scores for the Tennessee River calibration  
 960 region (see Fig. 9b for location). Orange is calibration, red is evaluation, and black is all years.

961

962

963

964

965

966

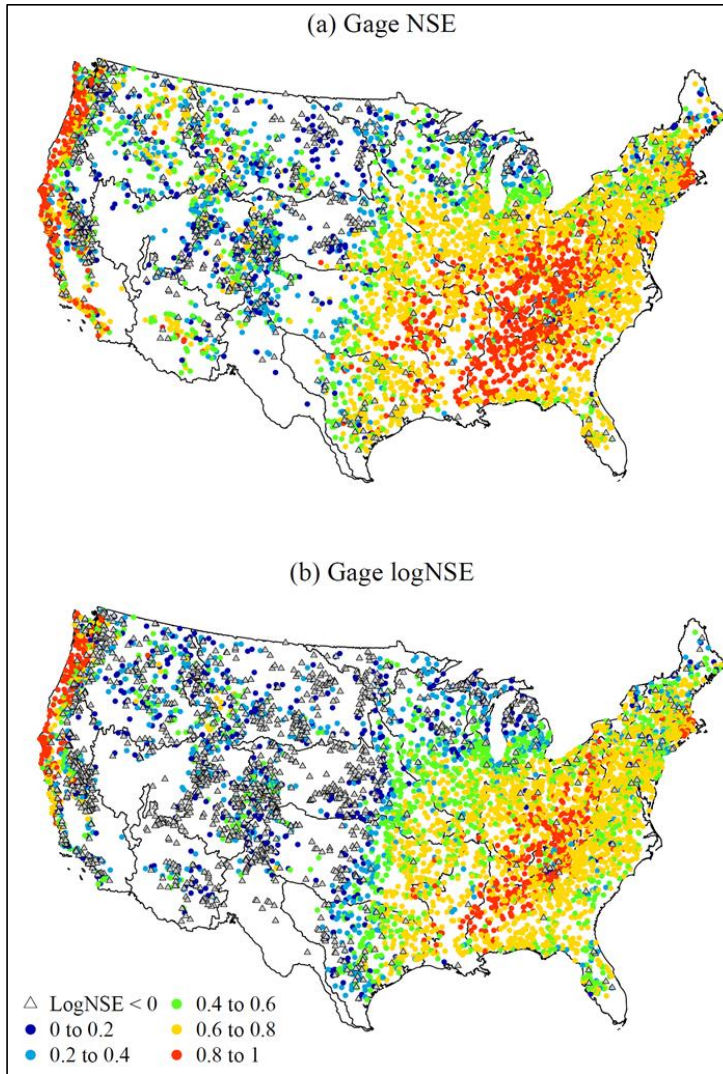
967

968

969

970

971

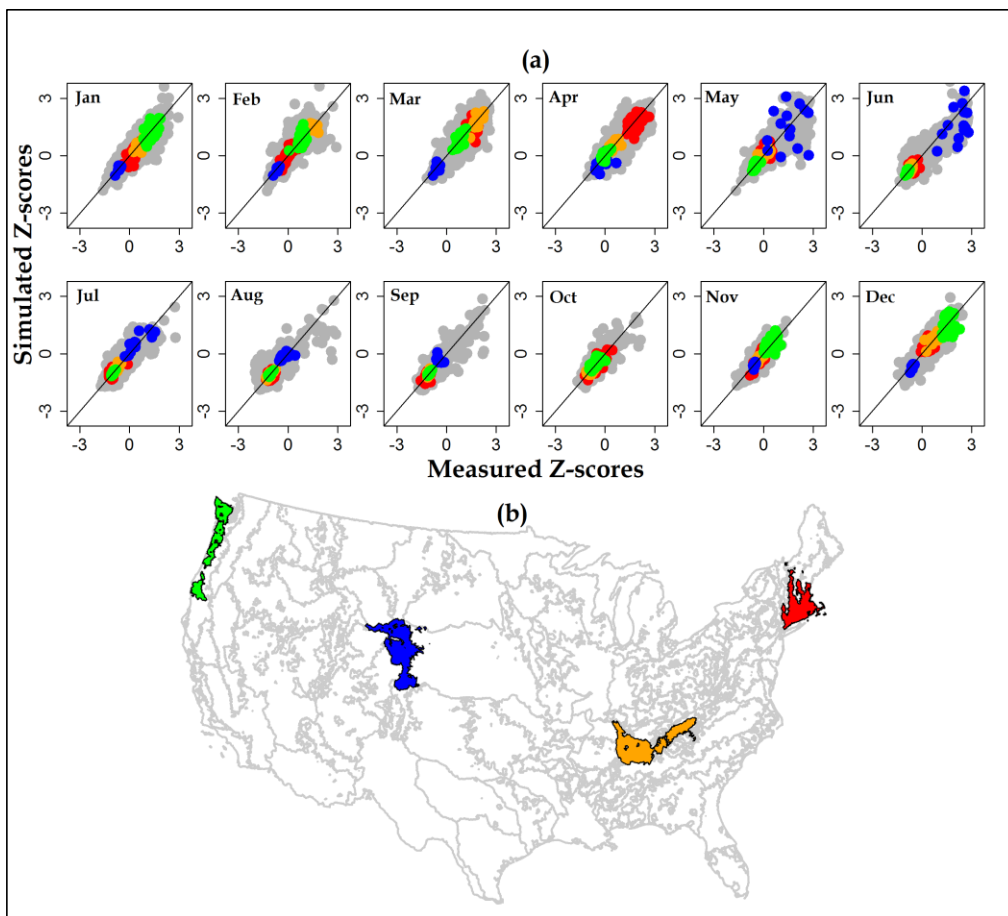


972

973 Figure 9. Individual streamgage calibration results: (a) Nash-Sutcliffe Efficiency (NSE)  
 974 coefficient and (b) log of the NSE (logNSE).

975

976



977

978 Figure 10. (a) Measured versus simulated mean monthly Z-scores for runoff at all streamgages

979 and (b) location of highlighted streamgages for four calibration regions: New England (67

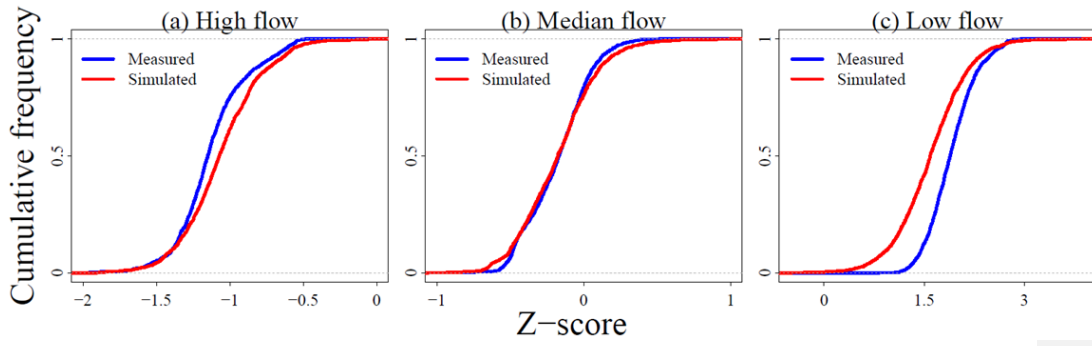
980 streamgages, red); Tennessee River (21 streamgages, orange); Platte Headwaters (15

981 streamgages, blue); and Pacific Northwest (33 streamgages, green).

982

983

984



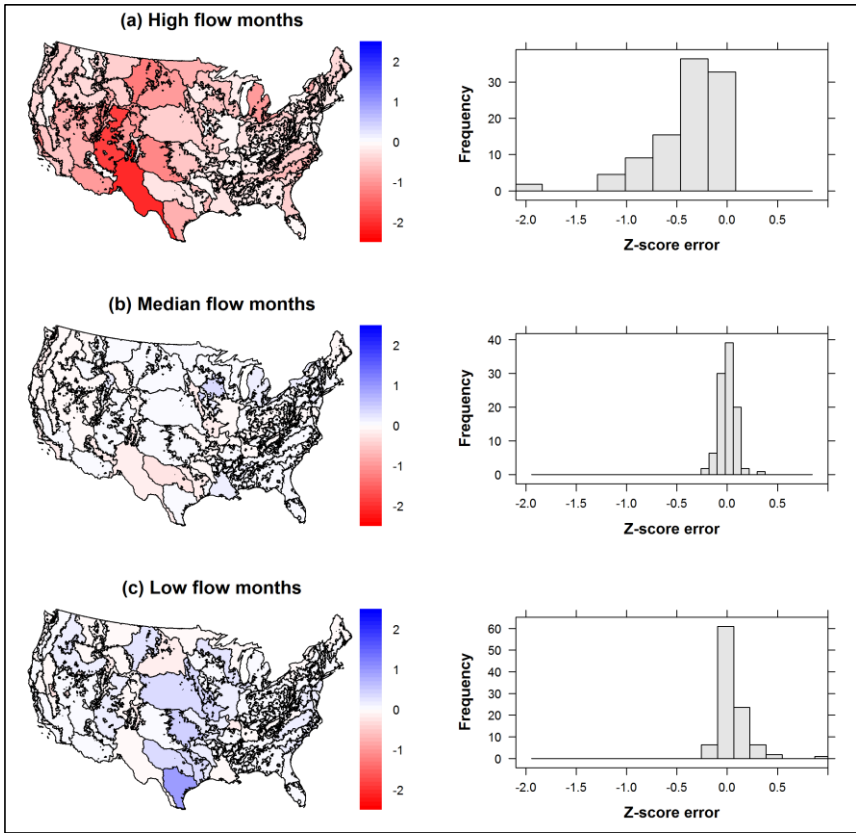
985

986 Figure 11. Z-score cumulative frequency for (a) highest-, (b) median-, and (c) lowest-flow

987

months.

988



989

990

991

992

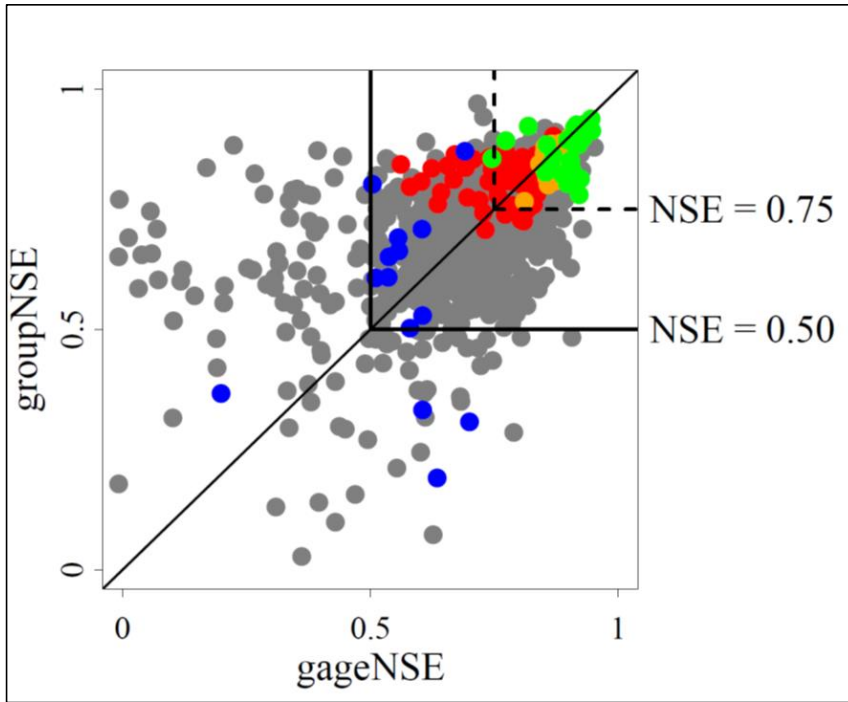
993

994

995

996

Figure 12. Z-score error (simulated - measured) for (a) highest-, (b) median-, and (c) lowest-flow months.



997

998

999

1000

1001

1002

1003

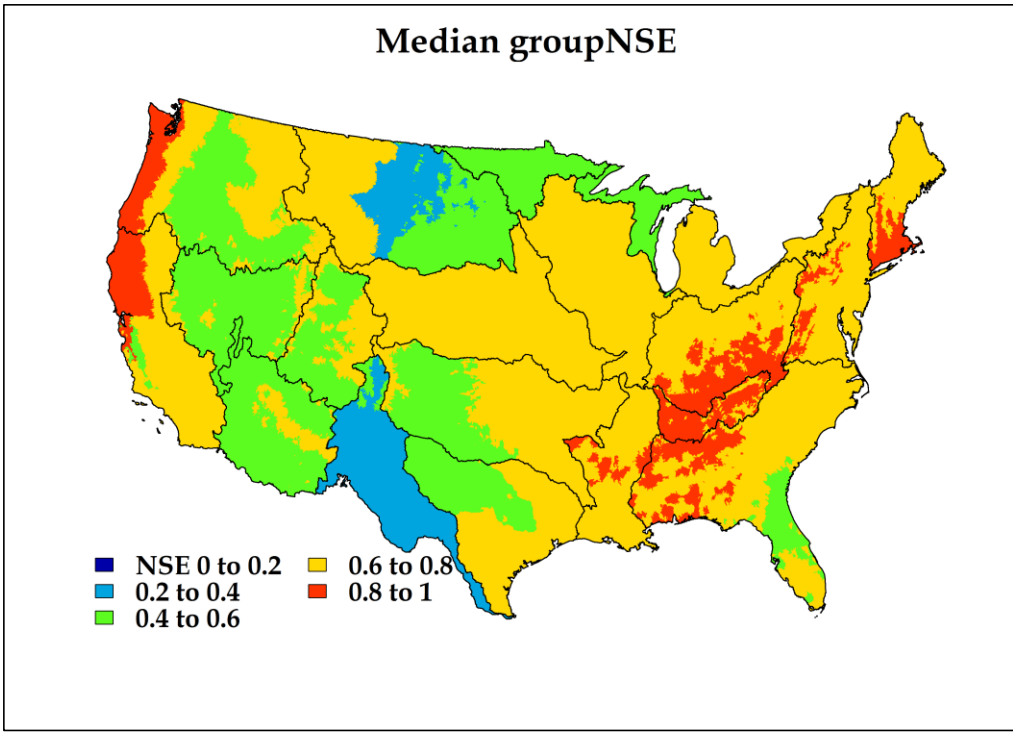
1004

1005

1006

Figure 13. Nash Sutcliffe Efficiency from individual (gageNSE) and grouped (groupNSE) calibration. Calibration regions in New England (67 streamgages, red); Tennessee River (21 streamgages, orange); Platte Headwaters (15 streamgages, blue); and Pacific Northwest (33 streamgages, green) are highlighted (see Fig. 9b for location).





1007

1008 Figure 14. Median Nash Sutcliffe Efficiency (NSE) of streamgages used for calibration by  
 1009 calibration region.

1010

1011